An initial study of mesons and baryons containing strange quarks with GlueX

(A proposal to the 40th Jefferson Lab Program Advisory Committee)

A. AlekSejevs,[1] S. Barkanova,[1] M. Dugger,[2] B. Ritchie,[2] I. Senderovich,[2] E. Anassontzis,[3] P. Ioannou,[3]
C. Kourkoumeli,[3] G. Voulgaris,[3] N. Jarvis,[4] W. Levine,[4] P. Mattione,[4] W. McGinley,[4] C. A. Meyer,[4, *]
R. Schumacher,[4] M. Staib,[4] P. Collins,[5] F. Klein,[5] D. Sober,[5] D. Doughty,[6] A. Barnes,[7] R. Jones,[7] J. McIntyre,[7]
F. Mokaya,[7] B. Pratt,[7] W. Boeglin,[8] L. Guo,[8] P. Khetarpal,[8] E. Pooser,[8] J. Reinhold,[8] H. Al Ghoul,[9] S. Capstick,[9]
V. Crede,[9] P. Eugenio,[9] A. Ostrovidov,[9] N. Sparks,[9] A. Tsaris,[9] D. Ireland,[10] K. Livingston,[10] D. Bennett,[11]
J. Bennett,[11] J. Frye,[11] M. Lara,[11] J. Leckey,[11] R. Mitchell,[11] K. Moriya,[11] M. R. Shepherd,[11, †] A. Szczepaniak,[11]
R. Miskimen,[12] A. Mushkarenkov,[12] J. Hardin,[13] J. Stevens,[13] M. Williams,[13] A. Ponosov,[14] S. Somov,[14]
C. Salgado,[15] P. Ambrozewicz,[16] A. Gasparian,[16] R. Pedroni,[16] T. Black,[17] L. Gan,[17] S. Dobbs,[18]
K. K. Seth,[18] A. Tomaradze,[18] J. Dudek,[19, 20] F. Close,[21] E. Swanson,[22] S. Denisov,[23] G. Huber,[24]
D. Kolybaba,[24] S. Krueger,[24] G. Lolos,[24] Z. Papandreou,[24] A. Semenov,[24] I. Semenova,[24] M. Tahani,[24]
W. Brooks,[25] H. Hakobyan,[25] S. Kuleshov,[25] O. Soto,[25] A. Toro,[25] I. Vega,[25] R. White,[25] F. Barbosa,[20]
E. Chudakov,[20, ‡] H. Egiyan,[20] M. Ito,[20] D. Lawrence,[20] M. McCaughan,[20] M. Pennington,[20] L. Pentchev,[20]
Y. Qiang,[20] E. S. Smith,[20] A. Somov,[20] S. Taylor,[20] T. Whitlatch,[20] E. Wolin,[20] and B. Zihlmann[20]

(The GlueX Collaboration)

[1] *Acadia University, Wolfville, Nova Scotia, B4P 2R6, Canada*
[2] *Arizona State University, Tempe, Arizona 85287, USA*
[3] *University of Athens, GR-10680 Athens, Greece*
[4] *Carnegie Mellon University, Pittsburgh, Pennsylvania 15213, USA*
[5] *Catholic University of America, Washington, D.C. 20064, USA*
[6] *Christopher Newport University, Newport News, Virginia 23606, USA*
[7] *University of Connecticut, Storrs, Connecticut 06269, USA*
[8] *Florida International University, Miami, Florida 33199, USA*
[9] *Florida State University, Tallahassee, Florida 32306, USA*
[10] *University of Glasgow, Glasgow G12 8QQ, United Kingdom*
[11] *Indiana University, Bloomington, Indiana 47405, USA*
[12] *University of Massachusetts, Amherst, Massachusetts 01003, USA*
[13] *Massachusetts Institute of Technology, Cambridge, Massachusetts 02139, USA*
[14] *MEPHI, Moscow, Russia*
[15] *Norfolk State University, Norfolk, Virginia 23504, USA*
[16] *North Carolina A&T State University, Greensboro, North Carolina 27411, USA*
[17] *University of North Carolina, Wilmington, North Carolina 28403, USA*
[18] *Northwestern University, Evanston, Illinois, 60208, USA*
[19] *Old Dominion University, Norfolk, Virginia 23529, USA*
[20] *Thomas Jefferson National Accelerator Facility, Newport News, Virginia 23606, USA*
[21] *University of Oxford, Oxford OX1 3NP, United Kingdom*
[22] *University of Pittsburgh, Pittsburgh, Pennsylvania 15260, USA*
[23] *Institute for High Energy Physics, Protvino, Russia*
[24] *University of Regina, Regina, SK S4S 0A2, Canada*
[25] *Universidad Técnica Federico Santa María, Casilla 110-V Valparaíso, Chile*

(Dated: May 2, 2013)

The primary motivation of the GlueX experiment is to search for and ultimately study the pattern of gluonic excitations in the meson spectrum produced in γp collisions. Recent lattice QCD calculations predict a rich spectrum of hybrid mesons that have both exotic and non-exotic J^{PC}, corresponding to $q\bar{q}$ states ($q = u$, d, or s) coupled with a gluonic field. A thorough study of the hybrid spectrum, including the identification of the isovector triplet, with charges 0 and ± 1, and both isoscalar members, $|s\bar{s}\rangle$ and $|u\bar{u}\rangle + |d\bar{d}\rangle$, for each predicted hybrid combination of J^{PC}, may only be achieved by conducting a systematic amplitude analysis of many different hadronic final states. Detailed studies of the performance of the GlueX detector have indicated that identification of particular final states with kaons is possible using the baseline detector configuration. The efficiency of kaon detection coupled with the relatively lower production cross section for particles containing hidden strangeness will require a high intensity run in order for analyses of such states to be feasible. We propose to collect a total of 200 days of physics analysis data at an average intensity of 5×10^7 tagged photons on target per second. This data sample will provide an order of magnitude statistical improvement over the initial GlueX running, which will allow us to begin a program of studying mesons and baryons containing strange quarks. In addition, the increased intensity will permit us to study reactions that may have been statistically limited in the initial phases of GlueX. Overall, this

will lead to a significant increase in the potential for GlueX to make key experimental advances in our knowledge of hybrid mesons and excited Ξ baryons.

I.   INTRODUCTION AND BACKGROUND

A long-standing goal of hadron physics has been to understand how the quark and gluonic degrees of freedom that are present in the fundamental QCD Lagrangian manifest themselves in the spectrum of hadrons. Of particular interest is how the gluon-gluon interactions might give rise to physical states with gluonic excitations. One class of such states is the hybrid meson, which can be naively thought of as a quark anti-quark pair coupled to a valence gluon ($q\bar{q}g$). Recent lattice QCD calculations [1] predict a rich spectrum of hybrid mesons. A subset of these hybrids has an unmistakable experimental signature: angular momentum (J), parity (P), and charge conjugation (C) that cannot be created from just a quark-antiquark pair. Such states are called exotic hybrid mesons. The primary goal of the GlueX experiment in Hall D is to search for and study these mesons.

A detailed overview of the motivation for the GlueX experiment as well as the design of the detector and beamline can be found in the initial proposal to the Jefferson Lab Program Advisory Committee (PAC) 30 [2], a subsequent PAC 36 update [3] and a conditionally approved proposal to PAC 39 [4]. While the currently-approved 120 days of beam time with the baseline detector configuration will allow GlueX an unprecedented opportunity to search for exotic hybrid mesons, the statistics that will be collected during this period will be inadequate for studying mesons or baryons containing strange quarks. These issues were addressed in our proposal to PAC 39 [4], where we proposed a complete package that would allow us to fully explore the strangeness sector using a combination of new particle-identification capability and the full implementation of our level-three (software) trigger to increase the data-rate capabilities of the experiment. This full functionality will ultimately be needed for the GlueX experiment to complete its primary goal of solidifying our experimental understanding of hybrids by identifying *patterns* of hybrid mesons, both isoscalar and isovector, exotic and non-exotic, that are embedded in the spectrum of conventional mesons. However, there are select final states containing strange particles that can be studied with the baseline GlueX equipment provided that the statistical precision of the data set is sufficient. This proposal focuses on those parts of the GlueX program that can be addressed with the baseline hardware, but will be statistically limited in the currently-approved GlueX running time. The motivation and experimental context for these studies is largely

the same as presented in our PAC 39 proposal; we repeat it here for completeness.

A.   Theoretical context

Our understanding of how gluonic excitations manifest themselves within QCD is maturing thanks to recent results from lattice QCD. This numerical approach to QCD considers the theory on a finite, discrete grid of points in a manner that would become exact if the lattice spacing were taken to zero and the spatial extent of the calculation, *i.e.,* the "box size," was made large. In practice, rather fine spacings and large boxes are used so that the systematic effect of this approximation should be small. The main limitation of these calculations at present is the poor scaling of the numerical algorithms with decreasing quark mass - in practice most contemporary calculations use a range of artificially heavy light quarks and attempt to observe a trend as the light quark mass is reduced toward the physical value. Trial calculations at the physical quark mass have begun and regular usage is anticipated within a few years.

The spectrum of eigenstates of QCD can be extracted from correlation functions of the type $\langle 0|\mathcal{O}_f(t)\mathcal{O}_i^\dagger(0)|0\rangle$, where the $\mathcal{O}^\dagger$ are composite QCD operators capable of interpolating a meson or baryon state from the vacuum. The time-evolution of the Euclidean correlator indicates the mass spectrum ($e^{-m_{\mathfrak{n}}t}$) and information about quark-gluon substructure can be inferred from matrix-elements $\langle\mathfrak{n}|\mathcal{O}^\dagger|0\rangle$. In a series of recent papers [5–8], the Hadron Spectrum Collaboration has explored the spectrum of mesons and baryons using a large basis of composite QCD interpolating fields, extracting a spectrum of states of determined $J^{P(C)}$, including states of high internal excitation.

As shown in Fig. 1, these calculations, for the first time, show a clear and detailed spectrum of exotic J^{PC} mesons, with a lightest 1^{-+} lying a few hundred MeV below a 0^{+-} and two 2^{+-} states. Beyond this, through analysis of the matrix elements $\langle\mathfrak{n}|\mathcal{O}^\dagger|0\rangle$ for a range of different quark-gluon constructions, $\mathcal{O}$, we can infer [1] that although the bulk of the non-exotic J^{PC} spectrum has the expected systematics of a $q\bar{q}$ bound state system, some states are only interpolated strongly by operators featuring non-trivial gluonic constructions. One may interpret these states as non-exotic hybrid mesons, and, by combining them with the spectrum of exotics, it is then possible to isolate a lightest hybrid supermultiplet of $(0, 1, 2)^{-+}$ and 1^{--} states, roughly 1.3 GeV heavier than the ρ meson. The form of the operator that has strongest overlap onto these states has an S-wave $q\bar{q}$ pair in a color octet configuration and an exotic gluonic field in a color octet with $J_g^{P_g C_g} = 1^{+-}$, a *chromomagnetic*

configuration. The heavier $(0, 2)^{+-}$ states, along with some positive parity non-exotic states, appear to correspond to a P-wave coupling of the $q\bar{q}$ pair to the same chromomagnetic gluonic excitation.

A similar calculation for isoscalar states uses both $u\bar{u} + d\bar{d}$ and $s\bar{s}$ constructions and is able to extract both the spectrum of states and also their hidden flavor mixing. (See Fig. 1.) The basic experimental pattern of significant mixing in 0^{-+} and 1^{++} channels and small mixing elsewhere is reproduced, and, for the first time, we are able to say something about the degree of mixing for exotic-J^{PC} states. In order to probe this mixing experimentally, it is essential to be able to reconstruct decays to both strange and non-strange final state hadrons.

A chromomagnetic gluonic excitation can also play a role in the spectrum of baryons: constructions beyond the simple qqq picture can occur when three quarks are placed in a color octet coupled to the chromomagnetic excitation. The baryon sector offers no "smoking gun" signature for hybrid states, as all J^P can be accessed by three quarks alone, but lattice calculations [8] indicate that there are "excess" nucleons with $J^P = 1/2^+$, $3/2^+$, $5/2^+$ and excess Δ's with $J^P = 1/2^+, 3/2^+$ that have a hybrid component. An interesting observation that follows from this study is that there appears to be a common energy cost for the chromomagnetic excitation, regardless of whether it is in a meson or baryon. In Fig. 2 we show the hybrid meson spectrum alongside the hybrid baryon spectrum with the quark mass contribution subtracted (approximately, by subtracting the ρ mass from the mesons, and the nucleon mass from the baryons). We see that there appears to be a common scale ~ 1.3 GeV for the gluonic excitation, which does not vary significantly with varying quark mass.

Hybrid baryons will be challenging to extract experimentally because they lack "exotic" character, and can only manifest themselves by overpopulating the predicted spectrum with respect to a particular model. The current experimental situation of nucleon and Δ excitations is, however, quite contrary to the findings in the meson sector. Fewer baryon resonances are observed than are expected from models using three symmetric quark degrees of freedom, which does not encourage adding additional gluonic degrees of freedom. The current experimental efforts at Jefferson Lab aim to identify the relevant degrees of freedom which give rise to nucleon excitations.

Lattice calculations have made great progress at predicting the N^* and Δ spectrum, including hybrid baryons [8, 9], and calculations are emerging for Ξ and Ω resonances [10]. Experimentally, the properties of these multi-strange states are poorly known; only the J^P of the $\Xi(1820)$ has been (directly) determined [11]. Previous experiments searching for Cascades were limited by low statistics and poor detector acceptance, making the interpretation of available data difficult. An experimental program on Cascade physics using the GLUEX detector provides a new window of opportunity in hadron spectroscopy and serves as a complementary approach to the challenging study of broad and overlapping N^* states. Furthermore, multi-strange baryons provide an important missing link between the light-flavor and the heavy-flavor baryons.

B. Experimental context

GLUEX is ideally positioned to conduct a search for light-quark exotics and provide complementary data on the spectrum of light-quark mesons. It is anticipated that between now and the time GLUEX begins data taking, many results on the light-quark spectrum will have emerged from the BESIII experiment, which is currently attempting to collect about 10^8 to 10^9 J/ψ and ψ' decays. These charmonium states decay primarily through $c\bar{c}$ annihilation and subsequent hadronization into light mesons, making them an ideal place to study the spectrum of light mesons. In fact several new states have already been reported by the BESIII collaboration such as the $X(1835)$, $X(2120)$, and $X(2370)$ in $J/\psi \to \gamma X$, $X \to \eta'\pi\pi$ [12]. No quantum number assignment for these states has been made yet, so it is not yet clear where they fit into the meson spectrum. GLUEX can provide independent confirmation of the existence of these states in a completely different production mode, in addition to measuring (or confirming) their J^{PC} quantum numbers. This will be essential for establishing the location of these states in the meson spectrum. The BESIII experiment has the ability to reconstruct virtually any combination of final state hadrons, and, due to the well-known initial state, kinematic fitting can be used to effectively eliminate background. The list of putative new states and, therefore, the list of channels to explore with GLUEX, is expected to grow over the next few years as BESIII acquires and analyzes its large samples of charmonium data.

While the glue-rich $c\bar{c}$ decays of charmonium have long been hypothesized as the ideal place to look for glueballs, decays of charmonium have also recently been used to search for exotics. The CLEO-c collaboration studied both $\pi^+\pi^-$ and $\eta'\pi^\pm$ resonances in the decays of $\chi_{c1} \to \eta'\pi^+\pi^-$ and observed a significant signal for an exotic 1^{-+} amplitude in the $\eta'\pi^\pm$ system [13]. The observation is consistent with the $\pi_1(1600)$ previously reported by E852 in the $\eta'\pi$ system [14]. However, unlike E852, the CLEO-c analysis was unable to perform a model-independent extraction of the $\eta'\pi$ scattering amplitude and phase to validate the resonant nature of the 1^{-+} amplitude. A similar analysis of χ_{c1} decays will most likely be performed by BESIII; however, even with an order of magnitude more data, the final $\eta'\pi^+\pi^-$ sample is expected to be just tens of thousands of events, significantly less than the proposed samples that will be collected with GLUEX. With the exception of this recent result from CLEO-c, the picture in the light quark exotic sector, and the justification for building GLUEX, remains largely the same as it did at the time of the original GLUEX pro-
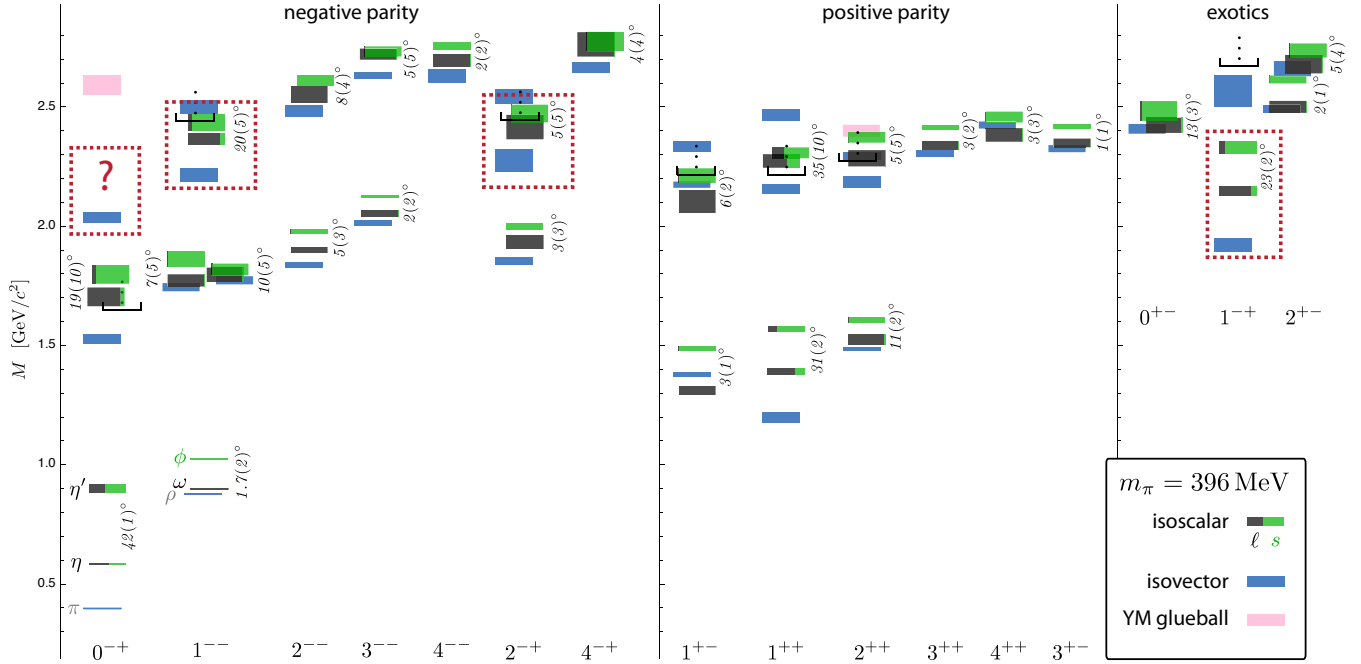
FIG. 1. A compilation of recent lattice QCD computations for both the isoscalar and isovector light mesons from Ref. [1], including $\ell\bar{\ell}$ $\left(|\ell\bar{\ell}\rangle \equiv (|u\bar{u}\rangle + |d\bar{d}\rangle)/\sqrt{2}\right)$ and $s\bar{s}$ mixing angles (indicated in degrees). The dynamical computation is carried out with two flavors of quarks, light (ℓ) and strange (s). The s quark mass parameter is tuned to match physical $s\bar{s}$ masses, while the light quark mass parameters are heavier, giving a pion mass of 396 MeV. The black brackets with upward ellipses represent regions of the spectrum where present techniques make it difficult to extract additional states. The dotted boxes indicate states that are interpreted as the lightest hybrid multiplet – the extraction of clear 0^{-+} states in this region is difficult in practice.
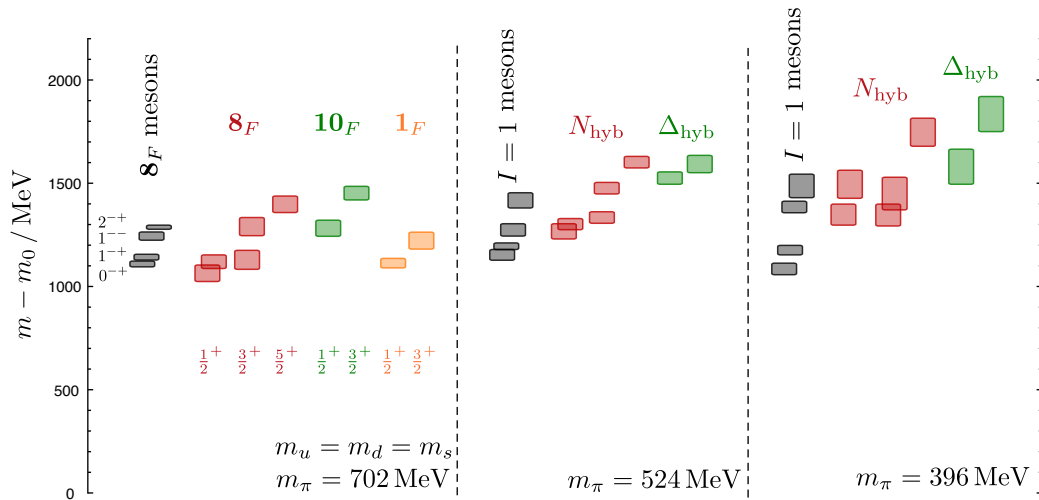

FIG. 2. Spectrum of gluonic excitations in hybrid mesons (gray) and hybrid baryons (red, green, and orange) for three light quark masses. The mass scale is $m - m_\rho$ for mesons and $m - m_N$ for baryons to approximately subtract the effect of differing numbers of quarks. The left calculation is performed with perfect $SU(3)$-flavor symmetry, and hybrid members of the flavor octets (8_F), decuplet (10_F), and singlet (1_F) are shown. The middle and right calculations are performed with a physical $s\bar{s}$ mass and two different values of m_π.

posal; see Ref. [15] for a review. All exotic candidates reported to date are isovector 1^{-+} states (π_1). By systematically exploring final states with both strange and non-strange particles, GLUEX will attempt to establish not just one exotic state, but a *pattern* of hybrid states with both exotic and non-exotic quantum numbers.

The idea that hybrids should also appear as supernumerary states in the spectrum of non-exotic J^{PC} mesons suggests an interesting interpretation of recent data in charmonium. Three independent experiments have observed a state denoted $Y(4260)$ [16–19]; it has 1^{--} quantum numbers but has no clear assignment in the arguably well-understood spectrum of $c\bar{c}$. Even though the state is above the $D\bar{D}$ mass threshold, it does not decay strongly to $D\bar{D}$ as the other 1^{--} $c\bar{c}$ states in that region do. Its mass is about 1.2 GeV above the ground state J/ψ, which is similar to the splitting observed in lattice calculations of light mesons and baryons. If this state is a non-exotic hybrid, an obvious, but very challenging, experimental goal would be to identify the exotic 1^{-+} $c\bar{c}$ hybrid member of the same multiplet, which should have approximately the same mass[1]. It is not clear how to produce such a state with existing experiments. In the light quark sector, some have suggested that the recently discovered $Y(2175)$ [20–22] is the strangeonium ($s\bar{s}$) analogue of the $Y(4260)$. If this is true, GLUEX is well-positioned to study this state and search for its exotic counterpart. We discuss this further in Section III B.

Recent CLAS results [23, 24] also suggest many opportunities to make advances in baryon spectroscopy. The CLAS collaboration investigated Ξ photoproduction in the reactions $\gamma p \to K^+ K^+ (X)$ as well as $\gamma p \to K^+ K^+ \pi^- (X)$ and, among other things, determined the mass splitting of the ground state (Ξ^-, Ξ^0) doublet to be 5.4 ± 1.8 MeV/c^2, which is consistent with previous measurements. Moreover, the differential cross sections for the production of the Ξ^- have been determined in the photon energy range from 2.75 to 3.85 GeV [24]. The cross section results are consistent with a production mechanism of $Y^* \to \Xi^- K^+$ through a t-channel process. The reaction $\gamma p \to K^+ K^+ \pi^- [\Xi^0]$ was also studied in search of excited Ξ resonances, but no significant signal for an excited Ξ state, other than the $\Xi^-(1530)$, was observed. The absence of higher-mass signals is very likely due to the low photon energies and the limited acceptance of the CLAS detector. With higher photon beam energy and two orders of magnitude more statistics, the GLUEX experiment will be well-suited to search for and study these excited Ξ resonances.

---

[1] Like the light quark mesons discussed in Sec. I A, the expectation for charmonium is that a 1^{--} non-exotic hybrid would exist with about the same mass as the 1^{-+} exotic charmonium hybrid [25, 26].

II. STATUS OF THE GLUEX EXPERIMENT

In the following section, we discuss the current status of the development of the baseline GLUEX experiment. The GLUEX experiment was first presented to PAC 30 in 2006 [2]. While beam time was not awarded for 12 GeV proposals at that PAC, the proposal suggested a three phase startup for GLUEX, which spanned approximately the first two calendar years of operation. Phase I covered detector commissioning. Phases II and III proposed a total of 7.5×10^6 s of detector live time at a flux of 10^7 γ/s for physics commissioning and initial exploratory searches for hybrid mesons. In 2010, an update of the experiment was presented to PAC 36 and a total of 120 days of beam time was granted for Phases I-III.

In 2008, two critical detector components were "descoped" from the design due to budgetary restrictions. First, and most importantly, the forward Cherenkov particle identification system was removed. The other component that was taken out was the level-three software trigger, which is needed for operating at a photon flux greater than 10^7 γ/s. These changes severely impact the ultimate scientific goals and discovery potential of the GLUEX experiment, as was noted in the PAC 36 report:

> Finally, the PAC would like to express its hope that the de-scoped Cherenkov detector be revisited at some time in the future. The loss of kaon identification from the current design is a real shame, but entirely understandable given the inescapable limitations on manpower, resources, and time.

In 2012, we proposed [4] both the implementation of the level-three trigger and the development of a kaon-identification system to be used during high intensity ($> 10^7$ γ/s) running of GLUEX. As noted in that proposal, the improved particle identification and the higher beam intensity would allow for a systematic exploration of higher-mass $s\bar{s}$ states as well as doubly-strange Ξ baryons. In particular, identifying the $s\bar{s}$ members of the hybrid nonets and studying $s\bar{s}$ and $\ell\bar{\ell}$ ($|\ell\bar{\ell}\rangle \equiv (|u\bar{u}\rangle + |d\bar{d}\rangle)/\sqrt{2}$) mixing amongst isoscalar mesons are crucial parts of the overall GLUEX program that would be fully addressed by the PAC 39 proposal. The PAC 39 proposal was conditionally approved, pending a final design of the kaon-identification system.

During the last twelve months, the collaboration has worked to better understand the kaon identification capability of the baseline equipment, in addition to examining how various additional particle identification detectors may augment this capability as we work towards the goals of our PAC 39 proposal. The level of detail with which we are now able to simulate the detector and carry out complex analysis tasks has improved dramatically. While we are still converging on a hardware design for a kaon identification system, our studies have revealed that an increase in intensity and running time alone is suffi-

cient to *begin* a program of studying mesons and baryons with hidden and open strangeness.

A. GlueX construction progress

A schematic view of the GlueX detector is shown in Fig. 3. The civil construction of Hall D is complete and the collaboration gained control of both Hall D and the Hall D tagger hall in 2012. Many of the detector components are now being installed, with others being tested prior to installation. As of April 2013, all major subdetector systems are either built or are under construction at Jefferson Lab or various collaborating institutions. Beam for the experiment will be derived from coherent bremsstrahlung radiation from a thin diamond wafer and delivered to a liquid hydrogen target. The solenoidal detector has both central and forward tracking chambers as well as central and forward calorimeters. Timing and triggering are aided by a forward time of flight wall and a thin scintillator start counter that encloses the target. We briefly review the capabilities and construction status of each of the detector components below. Table I lists all of the GlueX collaborating experimental institutions and their primary responsibilities. The collaboration consists of over a hundred members, including representation from the theory community.

1. Beamline and Tagger

The GlueX photon beam originates from coherent bremsstrahlung radiation produced by the 12 GeV electron beam impinging on a 20 μm diamond wafer. Orientation of the diamond and downstream collimation produce a photon beam peaked in energy around 9 GeV with about 40% linear polarization. A coarse tagger tags a broad range of electron energy, while precision tagging in the coherent peak is performed by a tagger microscope. A downstream pair spectrometer is utilized to measure photon conversions and determine the beam flux. Construction of the full system is underway.

Substantial work has also been done by the Connecticut group to fabricate and characterize thin diamond radiators for GlueX. This has included collaborations with the Cornell High Energy Synchrotron Source as well as industrial partners. Successful fabrication of 20 μm diamond radiators for GlueX has been demonstrated using a laser-ablation system at Connecticut. This system starts with a much thicker diamond wafer and thins the central part of the diamond down to the 20 μm thickness, leaving a thicker picture frame around the outside of the diamond. This frame allows for easier mounting and limits the vibration seen in thin diamonds. The design of the goniometer system to manipulate the diamond has been completed by the Glasgow group and has been ordered from private industry.

The tagger magnet and vacuum vessel are currently being installed in the Hall D tagger hall. The design for the precision tagger "microscope" was developed at Connecticut, including the custom electronics for silicon photomultiplier (SiPM) readout. Beam tests of prototypes have been conducted, and the construction of the final system is underway at Connecticut. The coarse tagger, which covers the entire energy range up to nearly the endpoint, is currently being built by the Catholic University group.

The groups from the University of North Carolina at Wilmington, North Carolina A&T State, and Jefferson Lab are collaborating to construct the pair spectrometer. A magnet obtained from Brookhaven has been modified to make it suitable for use in Hall D and is ready for installation. In addition, the Arizona State and Glasgow groups are collaborating to develop a technique for accurately measuring the linear polarization of the beam. Tests are planned in Mainz this year.

2. Solenoid Magnet

At the heart of the GlueX detector is the 2.2 T superconducting solenoid, which provides the essential magnetic field for tracking. The solenoidal geometry also has the benefit of reducing electromagnetic backgrounds in the detectors since low energy e^+e^- pairs spiral within a small radius of the beamline. The field is provided by four superconducting coils. These four coils have been tested independently with three of the four having been tested up to the nominal current of 1500 A while the remaining coil was only tested to 1200 A due to a problem with power leads that was unrelated to the coil itself. No serious problems were found. The magnet has now been fully assembled, and, in April 2013, the solenoid was successfully operated at 1500 A inside of Hall D.

3. Tracking

Charged particle tracking is performed by two systems: a central straw-tube drift chamber (CDC) and four six-plane forward drift chamber (FDC) packages. The CDC is composed of 28 layers of 1.5-m-long straw tubes. The chamber provides $r - \phi$ measurements for charged tracks. Sixteen of the 28 layers have a 6° stereo angle to supply z measurements. Each FDC package is composed of six planes of anode wires. The cathode strips on either side of the anode cross at ±75° angles, providing a two-dimensional intersection point on each plane. The construction of the CDC [27] has been completed by Carnegie Mellon University (CMU) and the chamber is currently being tested prior to delivery and installation in Hall D late in 2013. The construction of the FDC by Jefferson Lab is also complete, and the chamber packages are undergoing testing prior to installation in Hall D in the fall of 2013. The position resolution of the CDC and
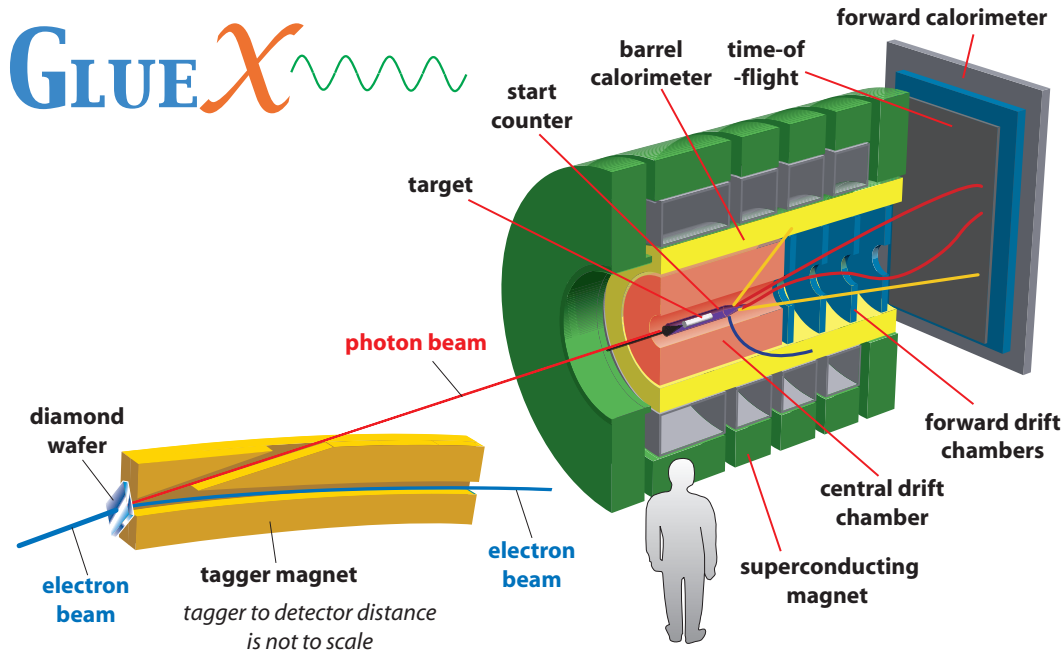
FIG. 3. A schematic of the GLUEX detector and beam.

FDC is about 150 μm and 200 μm, respectively. Together the approximate momentum resolution is 2%, averaged over the kinematical regions of interest.

Construction on the CDC began in May of 2010 with initial procurement and quality assurance of components and the construction of a 400 ft^2 class 2000 cleanroom at CMU. In August of that year, the end plates were mounted on the inner shell and then aligned. The empty frame was then moved into a vertical position for the installation of the 3522 straw tubes. This work started in November of 2010 and continued until October of 2011, when the outer shell was installed on the chamber. Stringing of the wires was completed in February of 2012, and all tension voltage and continuity checks were completed in March of 2012. In May of 2012, the upstream gas plenum was installed on the chamber and wiring of the high-voltage system commenced. This latter work finished in early 2013 at which point the chamber was checked for gas tightness and the down-stream gas window was installed.

After successful studies with a full-scale prototype, the FDC construction started in the beginning of 2011, with the entire production process carried out by Jefferson Lab in an off-site, 2000 ft^2 class 10,000 cleanroom. As of early 2013, all four packages had been completed and a spare is being constructed using the extra parts. Tests of the packages are being carried out with cosmic rays in a system that uses external chambers for tracking, scintillators for triggering, and a DAQ system. With the anticipated delivery of the needed flash-ADC modules in 2013, full package readout tests will be carried out. The chamber is scheduled to be installed in the fall of 2013.

4. Calorimetry

Like tracking, the GLUEX calorimetry system consists of two detectors: a barrel calorimeter with a cylindrical geometry (BCAL) and a forward lead-glass calorimeter with a planar geometry (FCAL). The primary goal of these systems is to detect photons that can be used to reconstruct π^0's and η's, which are produced in the decays of heavier states. The BCAL is a relatively high-resolution sampling calorimeter, based on 1 mm double-clad Kuraray scintillating fibers embedded in a lead matrix. It is composed of 48 four-meter-long modules; each module having a radial thickness of 15.1 radiation lengths. Modules are read out on each end by silicon SiPMs, which are not adversely affected by the high magnetic field in the proximity of the GLUEX solenoid flux return. The forward calorimeter is composed of 2800 lead glass modules, stacked in a circular array. Each bar is coupled to a conventional phototube. The fractional energy resolution of the combined calorimetry system $\delta(E)/E$ is approximately 5%-6%/$\sqrt{E \ [\text{GeV}]}$. Monitoring systems for both detectors have been designed by the group from the University of Athens.

All 48 BCAL calorimeter modules and a spare have been fabricated by the University of Regina and are at Jefferson Lab where they have been fitted with light guides and sensors. The modules are currently being installed in the GlueX detector. These light guides were fabricated at the University of Santa María (USM), which was also responsible for testing of most of the Hamamatsu S12045X MPPC arrays (SiPMs). The LED cali-

TABLE I. A summary of GLUEX institutions and their responsibilities.

Institution	Responsibilities
Arizona State U.	beamline polarimetry, beamline support
Athens	BCAL and FCAL calibration
Carnegie Mellon U.	CDC, offline software, management
Catholic U. of America	tagger system
Christopher Newport U.	trigger system
U. of Connecticut	tagger microscope, diamond targets, offline software
Florida International U.	start counter
Florida State U.	TOF system, offline software
U. of Glasgow	goniometer, beamline support
Indiana U.	FCAL, offline software, management
Jefferson Lab	FDC, data acquisition, trigger, electronics, infrastructure, management
U. of Massachusetts	target, electronics testing
Massachusetts Institute of Technology	level-3 trigger, forward PID, offline software
MEPHI	offline and online software
Norfolk State U.	installation and commissioning
U. of North Carolina A&T State	beamline support
U. of North Carolina, Wilmington	pair spectrometer
Northwestern U.	detector calibration
U. Técnica Federico Santa María	BCAL readout
U. of Regina	BCAL, SiPM testing

bration system for the BCAL was built by the University of Athens and has been installed as well.

The 2800 lead glass modules needed for the FCAL have been assembled at Indiana University and shipped to Jefferson Lab. They are now stacked in the detector frame in Hall D, and work is proceeding on the remaining infrastructure and cabling to support the readout of the detector. All of the PMTs are powered by custom-built Cockcroft-Walton style photomultiplier bases [28] in order to reduce cable mass, power dissipation, and high voltage control system costs. The design, fabrication, and testing of the bases was completed at Indiana University. In addition, a 25-block array utilizing the production design of all FCAL components was constructed and tested with electrons in Hall B by the Indiana University group in the spring of 2012; results indicate that the performance meets or exceeds expectations [29].

5. Particle ID and timing

The particle ID capabilities of GLUEX are derived from several subsystems. A dedicated forward time-of-flight wall (TOF), which is constructed from two planes of 2.5-cm-thick scintillator bars, provides about 70 ps timing resolution on forward-going tracks within about 10° of the beam axis. This information is complemented by time-of-flight data from the BCAL and specific ionization (dE/dx) measured with the CDC, both of which are particularly important for identifying the recoil proton in $\gamma p \to X p$ reactions. Finally, identification of the beam bunch, which is critical for timing measurements, is performed by a thin start counter that surrounds the target.

The TOF system is currently under construction at Florida State University. A prototype built using the final design hardware has achieved 100 ps resolution for mean time from a single counter read-out from both ends. The system consists of two planes of such counters, implying that the demonstrated two-plane resolution is 70 ps. The detector is expected to be installed in Hall D late in 2013.

Engineering drawings for the start counter are under development. The counters and the electronics have to fit into a narrow space between the target vacuum chamber and the inner wall of the CDC. Prototypes have obtained a time resolution of 300 to 600 ps, depending on the position of the hit along the length of the counter. The final segmentation has been fixed. SiPMs will be used for readout because they can be placed in the high magnetic field environment very close to the counters, thereby preserving scintillation light. The design of the SiPM electronics is about to start, and a final prototype of the scintillator assembly is under development.

The combined PID system in the baseline design is sufficient for identification of most protons in the kinematic regions of interest for GLUEX. The forward PID can be used to enhance the purity of the charged pion sample. However, the combined momentum, path length, and timing resolution only allows for exclusive kaon identification for track momenta less than 2.0 GeV/c. How-

ever, because the hermetic GlueX detector often reconstructs all final state particles, one can test conservation of four-momentum via a kinematic fit as a means of particle identification. This is especially effective when the recoil nucleon is measured. While it is true that no single particle identification measurement in GlueX provides complete separation between kaons and pions, the contributions of many different but correlated measurements can provide effective PID.

B. GlueX software readiness

Jefferson Lab organized an external review of the software efforts in all aspects of the 12 GeV project in order to assess the status of software development in all experimental halls as well as identify any issues that would impede progress toward the 12 GeV physics goals. This review took place in June, 2012, and the report, issued in September [30], stated

> Overall, the Committee was very impressed with the current state of software and computing preparations and the plans leading up to 12 GeV data taking.

The sophistication of GlueX simulation and reconstruction software was positively received by the committee. The recommendations of the committee focused on large scale implementation of these tools on both large data sets and with large groups of people. Recommendations were:

- The data volume and processing scale of GlueX is substantial but plans for data management and workload management systems supporting the operational scale were not made clear. They should be carefully developed.

- A series of scale tests ramping up using JLab's LQCD farm should be planned and conducted.

The GlueX collaboration responded to both of these. To address the first recommendation and prepare for the second recommendation several steps were taken.

- The format for reconstructed GlueX data has been defined and implemented in all GlueX software. The size of the reconstructed data set is substantially smaller than the estimates made at the time of the software review and lead us to believe that it should be possible to keep GlueX data live on disk at multiple sites.

- The format for raw data has been developed in collaboration with the data acquisition group. The typical size of these events is about 50% of what was originally estimated, but there remains significant uncertainty in how much this size may be inflated by detector noise.

- To address analysis workload management, we have developed an analysis framework that allows high-level, uniform access to a standardized set of reconstructed data as well as a consistent interface to analysis tasks such as kinematic fitting and particle identification code. Our intent is to make this a standard platform that facilitates easy analysis of any reaction by any member of the collaboration.

With this new infrastructure, the collaboration conducted a data challenge in December 2012, where over 5×10^9 γp inclusive hadronic physics events were simulated and reconstructed. The point of this effort was not only to generate a large data sample for physics studies, but to also stress the robustness and throughput capability of the current GlueX software at scales comparable to production running, in line with the committee recommendation. The five-billion event sample represents more than half of what will be collected in a year of Phase III GlueX running ($10^7 \gamma/s$). These events were simulated and reconstructed on a combination of the Open-science Grid (OSG) (4×10^9 events), the Jefferson Lab farm (1×10^9 events) and the Carnegie Mellon computer cluster (0.3×10^9 events). We plan to incorporate the lessons learned from this data challenge into another similar exercise later this year.

It is this large data sample, coupled with smaller samples of specific final states and new sophisticated analysis tools, that has allowed us to better understand the performance and capabilities of the baseline GlueX detector. This ultimately has given us confidence that the baseline GlueX detector is capable of carrying out initial studies of the $s\bar{s}$ hybrid spectrum for a select number of final states.

C. Sensitivity and limitations to physics goals during initial GlueX running

1. Initial GlueX physics goals: non-strange final states

Phases I-III of the GlueX physics program provide an excellent opportunity for both the study of conventional mesons and the search for exotic mesons in photoproduction. When one considers both production cross sections and detection efficiencies, the final states of interest will most likely focus on those decaying into non-strange mesons: π, η, η', and ω. Table III summarizes the expected lowest-mass exotics and possible decay modes. Initial searches will likely focus on the π_1 isovector triplet and the η_1 isoscalar. It will also be important to try to establish the other (non-exotic) members of the hybrid multiplet: the 0^{-+}, 1^{--}, and 2^{-+} states. Finally, the initial data may provide an opportunity to search for the heavier exotic b_2 and h_2 states.

One reaction of interest is $\gamma p \rightarrow \pi^+\pi^-\pi^+ n$. The $(3\pi)^{\pm}$ system has been studied extensively with data from E852 [31, 32] and COMPASS [33], with COMPASS
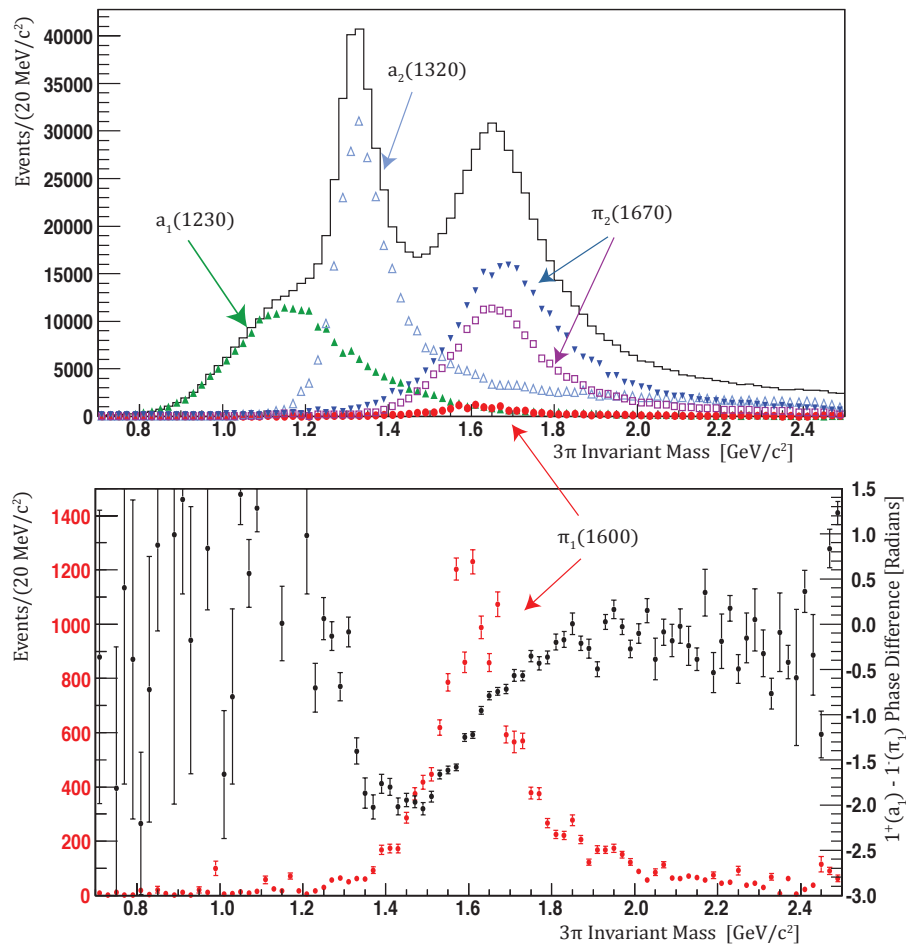
FIG. 4. A sample amplitude analysis result for the $\gamma p \rightarrow \pi^+\pi^-\pi^+ n$ channel with GLUEX. (top) The invariant mass spectrum as a function of $M(\pi^+\pi^-\pi^+)$ is shown by the solid histogram. The results of the amplitude decomposition into resonant components in each bin is shown with points and error bars. (bottom) The exotic amplitude, generated at a relative strength of 1.6%, is cleanly extracted (red points). The black points show the phase between the π_1 and a_1 amplitudes.

reporting evidence for the exotic $\pi_1(1600) \rightarrow \rho\pi$ decay. CLAS [34] has placed an upper limit on the photoproduction of the $\pi_1(1600)$ and the subsequent decay to $\rho\pi$. We have used this limit as a benchmark to test the GLUEX sensitivity to small amplitudes by performing an amplitude analysis on a sample of purely generated $\gamma p \rightarrow \pi^+\pi^-\pi^+ n$ events that has been subjected to full detector simulation and reconstruction as discussed above. Several conventional resonances, the a_1, π_2, and a_2, were generated along with a small ($< 2\%$) component of the exotic π_1. The result of the fit is shown in Figure 4; the exotic amplitude and its phase are clearly extracted.

GLUEX plans to systematically explore other non-strange channels, especially those that are predicted to be favorable hybrid decays. One such study is to search for hybrid decays to $b_1\pi$, which, considering the $b_1 \rightarrow \omega\pi$ decay, results in a $5\pi p$ final state. In an analysis of mock

data, we were able to use event selection and amplitude analysis to extract production of an exotic hybrid decay to $b_1\pi$ that is produced at a level corresponding to 0.03% of the total hadronic cross section [35]. The signal to background ratio for the $\omega\pi\pi p$ sample exceeded 10:1. Both of these studies indicate that the GLUEX detector provides excellent sensitivity to exotic mesons that decay into non-strange final states.

As detailed later, production cross sections for many of these non-strange topologies of interest are not well-known. Data from pion production experiments or branching fractions of heavy mesons suggest that production of η and especially η' might be suppressed. This implies that a high-statistics study of, for example, $\gamma p \rightarrow \eta'\pi^+ n$ to search for the exotic state reported by E852 [14] or a study of the $f_1\pi$ final state, which populates $\eta\pi\pi$, will likely need the data derived from the

high-intensity run put forth in this proposal.

2. GLUEX *sensitivity to final states with strangeness*

GLUEX does not contain any single detector element that is capable of providing discrimination of kaons from pions over the full-momentum range of interest for many key reactions. However, the hermetic GLUEX detector is capable of exclusively reconstructing all particles in the final state. In the case where the recoil nucleon is a proton that is detectable by the tracking chamber, this exclusive reconstruction becomes a particularly powerful tool for particle identification because conservation of four-momentum can be checked, via a kinematic fit, for various mass hypotheses for the final state particles. Many other detector quantities also give an indication of the particle mass, as assumptions about particle mass (pion or kaon) affect interpretation of raw detector information.

An incomplete list of potentially discriminating quantities include:

- The confidence level (CL) from kinematic fitting that the event is consistent with the desired final state.

- The CL(s) from kinematic fitting that the event is consistent with some other final states.

- The goodness of fit (χ^2) of the primary vertex fit.

- The goodness of fit (χ^2) of each individual track fit.

- The CL from the time-of-flight detector that a track is consistent with the particle mass.

- The CL from the energy loss (dE/dx) that a track is consistent with the particle type.

- The change in the goodness of fit ($\Delta\chi^2$) when a track is removed from the primary vertex fit.

- Isolation tests for tracks and the detected showers in the calorimeter system.

- The goodness of fit (χ^2) of possible secondary vertex fits.

- Flight-distance significance for particles such as K_S and Λ that lead to secondary vertices.

- The change in goodness of fit ($\Delta\chi^2$) when the decay products of a particle that produces a secondary vertex are removed from the primary vertex fit.

The exact way that these are utilized depends on the particular analysis, but it is generally better to try and utilize as many of these as possible in a collective manner, rather than simply placing strict criteria on any one of them. This means that we take advantage of correlations between variables in addition to the variables themselves.

One method of assembling multiple correlated measurements into a single discrimination variable is a boosted decision tree (BDT) [36].

Multivariate classifiers are playing an increasingly prominent role in particle physics. The inclusion of BDTs and artificial neural networks (ANNs) is now commonplace in analysis selection criteria. BDTs are now even used in software triggers [37, 38]. Traditionally, analyses have classified candidates using a set of variables, such as a kinematic fit confidence level, charged-particle time of flight, energy loss (dE/dx), *etc.*, where cuts are placed on each of the input variables to enhance the signal. In a BDT analysis, however, cuts on individual variables are not used; instead, a single classifier is formed by combining the information from all of the input variables.

The first step in constructing a decision tree (DT) is to split the data into two subsamples (of unequal size) using the input variable which gives the largest separation between signal and background. The variable to split on is determined by looping over all inputs. As a result of this split, one subsample should be mostly background and the other mostly signal. We now refer to these subsamples as branches. The process is repeated for these two branches, looping over all input variables to produce a second generation of four branches. The process is repeated again on this new generation of branches, and then again as necessary until the tree is complete. The final set of branches, referred to as *leaves*, is reached when one of the following occurs: a branch contains only signal or background events and so cannot be split any further; a branch has too few events to be split (a parameter specified by the grower of the tree); or the maximum number of total leaves has been reached (also a parameter specified by the grower). Correlations are exploited by ensuring that all the input variables are included each time, including those used in previous branch divisions.

The above process is carried out using a training data sample that consists of events (possibly simulated) where it is known which class, signal or background, each event belongs to. A single DT will overtrain and learn some fine-structure aspects of the data sample used for training which are due to statistical limitations of the data used and not aspects of the parent probability density function, *i.e.*, it will train on fluctuations. To counter this, a series of classifiers is trained which greatly enhances the performance. The training sample for each member of the series is augmented based on the performance of previous members. Incorrectly classified events are assigned larger weights or boosted in importance; this technique is referred to as boosting. The result is that each successive classifier is designed to improve the overall performance of the series in the regions where its predecessors have failed. In the end, the members of the series are combined to produce a single powerful classifier: a BDT. The performance is validated using an independent data sample, called a validation sample, that was not used in the training. If the performance is found to be similar when using the training (where it is maximally biased) and

validation (where it is unbiased) samples, then the BDT performance is predictable. Practically, the output of the BDT is a single number for each event that tends towards one for signal-like events but tends towards negative one for background-like events. Placing a requirement on the minimum value of this classifier, which incorporates all independent information input to the BDT, allows one to enhance the signal purity of a sample. For a pedagogical description of BDTs, see Ref. [39].

We illustrate the effectiveness of the BDT method by examining a reaction of the type

$$\gamma p \to p K^+ K^- \pi^+ \pi^-,$$

where we only consider the case where the recoil proton is reconstructed. A missing recoil nucleon reduces the number of constraints in the kinematic fit, and, consequently, dramatically diminishes the capability of the fit to discriminate pions from kaons. One can build a BDT for the reaction of interest, and look at the efficiency of selecting true signal events as a function of the sample purity. These studies do not include the efficiency of reconstructing the tracks in the detector, but start at the point where a candidate event containing five charged tracks has been found. Selection efficiencies are given in Table II. When coupled with estimates of the detection efficiency, these data suggest that it may be possible to have 90% pure kaon samples with an overall efficiency that is acceptable for analysis. We are limited to events where a recoil proton is detected, and, if we desire higher purity (lower background), then the efficiency drops dramatically.

TABLE II. The selection efficiency of the BDT method for physics channel leading to a $K^+ K^- \pi^+ \pi^- p$ final state, assuming a particular signal purity is desired. Efficiency is selection efficiency only and does not include reconstruction efficiency. The BDT method has been optimized using the simulation-determined GLUEX tracking resolution and a 50% degraded tracking resolution to account for potential resolution simulation errors.

Final State	Tracking Resolution	Signal Purity	Selection Efficiency
$K^+ K^- \pi^+ \pi^- p$	Nominal	0.90	0.26
$K^+ K^- \pi^+ \pi^- p$	Nominal	0.95	0.09
$K^+ K^- \pi^+ \pi^- p$	Degraded	0.90	0.25
$K^+ K^- \pi^+ \pi^- p$	Degraded	0.95	0.09

3. Limitations of existing kaon identification algorithms

It is important to point out that the use of kinematic constraints to achieve kaon identification, without dedicated hardware, has limitations. By requiring that the recoil proton be reconstructed, we are unable to study charge exchange processes that have a recoil neutron. In addition, this requirement results in a loss of efficiency

of 30%-50% for proton recoil topologies and biases the event selection to those that have high momentum transfer, which may make it challenging to conduct studies of the production mechanism. Our studies indicate that it will be difficult to attain very high purity samples with a multivariate analysis alone. In channels with large cross sections, the GLUEX sensitivity will not be limited by acceptance or efficiency, but by the ability to suppress and parameterize backgrounds in the amplitude analysis. To push the limits of sensitivity we need not only high statistics but high purity. Finally, it is worth noting that our estimates of the kaon selection efficiency using kinematic constraints depends strongly on our ability to model the performance of the detector. Although we have constructed a complete simulation, the experience of the collaboration with comparable detector systems indicates that the simulated performance is often better than the actual performance in unforeseen ways.

While the studies of kaon-identification systems as part of the PAC 39 proposal are not yet complete, some general comments can be made on the impact of additional kaon-identification. The obvious advantage of supplemental particle identification hardware is that it provides new, independent information to the multivariate analysis that has a very high discrimination power. We see noticeable improvements in efficiency when information from various design supplemental kaon ID systems is included in the BDT; this is especially dramatic at 95% purity.

Despite the limitations noted above, we will demonstrate that a program of high intensity running with the GLUEX detector, even without a dedicated particle identification upgrade, is capable of producing interesting results in the study of $s\bar{s}$ mesons and Ξ baryons. In addition, the order-of-magnitude increase in statistical precision in non-strange channels will allow us to study production mechanisms (t-dependence of reactions) with greater precision and to search for rarely produced resonances.

III. STUDY OF $s\bar{s}$ MESONS

The primary goal of the GLUEX experiment is to conduct a definitive mapping of states in the light meson sector, with an emphasis on searching for exotic mesons. Ideally, we would like to produce the experimental analogue of the lattice QCD spectrum pictured in Fig. 1, enabling a direct test of our understanding of gluonic excitations in QCD. In order to achieve this, one must be able to reconstruct strange final states, as observing decay patterns of mesons has been one of the primary mechanisms of inferring quark flavor content. An example of this can be seen by examining the two lightest isoscalar 2^{++} mesons in the lattice QCD calculation in Fig. 1. The two states have nearly pure flavors, with only a small (11°) mixing in the $\ell\bar{\ell}$ and $s\bar{s}$ basis. A natural experimental assignment for these two

states are the $f_2(1270)$ and the $f_2'(1525)$. An experimental study of decay patterns shows that $\mathcal{B}(f_2(1270) \to KK)/\mathcal{B}(f_2(1270) \to \pi\pi) \approx 0.05$ and $\mathcal{B}(f_2'(1525) \to \pi\pi)/\mathcal{B}(f_2'(1525) \to KK) \approx 0.009$ [11], which support the prediction of an $f_2(1270)$ ($f_2'(1525)$) with a dominant $\ell\bar{\ell}$ ($s\bar{s}$) component. By studying both strange and non-strange decay modes of mesons, GlueX hopes to provide similarly valuable experimental data to aid in the interpretation of the hybrid spectrum.

A. Exotic $s\bar{s}$ states

While most experimental efforts to date have focused on the lightest isovector exotic meson, the $J^{PC} = 1^{-+}$ $\pi_1(1600)$, lattice QCD clearly predicts a rich spectrum of both isovector and isoscalar exotics, the latter of which may have mixed $\ell\bar{\ell}$ and $s\bar{s}$ flavor content. A compilation of the "ground state" exotic hybrids is listed in Table III, along with theoretical estimates for masses, widths, and key decay modes. It is expected that initial searches with the baseline GlueX hardware will target primarily the π_1 state. Searches for the η_1, h_0, and b_2 may be statistically challenging, depending on the masses of these states and the production cross sections. With increased statistics and kaon identification, the search scope can be broadened to include these heavier exotic states in addition to the $s\bar{s}$ states: η_1', h_0', and h_2'. The η_1' and h_2' are particularly interesting because some models predict these states to be relatively narrow, and that they should decay through well-established kaon resonances.

The observation of various π_1 states has been reported in the literature for over fifteen years, with some analyses based on millions of events. However, it is safe to say that there exists a fair amount of skepticism regarding the assertion that unambiguous experimental evidence exists for exotic hybrid mesons. If the scope of exotic searches with GlueX is narrowed to only include the lightest isovector π_1 state, the ability for GlueX to comprehensively address the question of the existence of gluonic excitations in QCD is greatly diminished. On the other hand, clearly identification of all exotic members of the lightest hybrid multiplet, the three exotic $\pi_1^{\pm,0}$ states and the exotic η_1 and η_1', which can only be done by systematically studying a large number of strange and non-strange decay modes, would provide unambiguous experimental confirmation of exotic mesons. A study of decays to kaon final states could demonstrate that the η_1 candidate is dominantly $\ell\bar{\ell}$ while the η_1' candidate is $s\bar{s}$, as predicted by initial lattice QCD calculations. Such a discovery would represent a substantial improvement in the experimental understanding of exotics. In addition, further identification of members of the 0^{+-} and 2^{+-} nonets as well as measuring the mass splittings with the 1^{+-} states will validate the lattice QCD inspired phenomenological picture of these states as P-wave couplings of a gluonic field with a color-octet $q\bar{q}$ system.

B. Non-exotic $s\bar{s}$ mesons

As discussed in Section I A, one expects the lowest-mass hybrid multiplet to contain $(0, 1, 2)^{-+}$ states and a 1^{--} state that all have about the same mass and correspond to an S-wave $q\bar{q}$ pair coupling to the gluonic field in a P-wave. For each J^{PC} we expect an isovector triplet and a pair of isoscalar states in the spectrum. Of the four sets of J^{PC} values for the lightest hybrids, only the 1^{-+} is exotic. The other hybrid states will appear as supernumerary states in the spectrum of conventional mesons. The ability to clearly identify these states depends on having a thorough and complete understanding of the meson spectrum. Like searching for exotics, a complete mapping of the spectrum of non-exotic mesons requires the ability to systematically study many strange and non-strange final states. Other experiments, such as BESIII or COMPASS, are carefully studying this with very high statistics data samples and and have outstanding capability to cleanly study any possible final state. While the production mechanism of GlueX is complementary to that of charmonium decay or pion beam production and is thought to enhance hybrid production, it is essential that the detector capability and statistical precision of the data set be competitive with other contemporary experiments in order to maximize the collective experimental knowledge of the meson spectrum.

Given the recent developments in charmonium (briefly discussed in Section I B), a state that has attracted a lot of attention in the $s\bar{s}$ spectrum is the $Y(2175)$, which is assumed to be an $s\bar{s}$ vector meson (1^{--}). The $Y(2175)$ has been observed to decay to $\pi\pi\phi$ and has been produced in both J/ψ decays [21] and e^+e^- collisions [20, 22]. The state is a proposed analogue of the $Y(4260)$ in charmonium, a state that is also about 1.2 GeV heavier than the ground state triplet (J/ψ) and has a similar decay mode: $Y(4260) \to \pi\pi J/\psi$. The $Y(4260)$ has no obvious interpretation in the charmonium spectrum and has been speculated to be a hybrid meson [40–43], which, by loose analogy, leads to the implication that the $Y(2175)$ might also be a hybrid candidate. It should be noted that the spectrum of 1^{--} $s\bar{s}$ mesons is not as well-defined experimentally as the $c\bar{c}$ system; therefore, it is not clear that the $Y(2175)$ is a supernumerary state. However, GlueX is ideally suited to study this system. We know that vector mesons are copiously produced in photoproduction; therefore, with the ability to identify kaons, a precision study of the 1^{--} $s\bar{s}$ spectrum can be conducted with GlueX. Some have predicted [44] that the potential hybrid nature of the $Y(2175)$ can be explored by studying ratios of branching fractions into various kaonic final states. In addition, should GlueX be able to conclude that the $Y(2175)$ is in fact a supernumerary vector meson, then a search can be made for the exotic 1^{-+} $s\bar{s}$ member of the multiplet (η_1'), evidence of which would provide a definitive interpretation of the $Y(2175)$ and likely have implications on how one interprets charmonium data.

TABLE III. A compilation of exotic quantum number hybrid approximate masses, widths, and decay predictions. Masses are estimated from dynamical LQCD calculations with $M_\pi = 396$ MeV/c^2 [1]. The PSS (Page, Swanson and Szczepaniak) and IKP (Isgur, Kokoski and Paton) model widths are from Ref. [45], with the IKP calculation based on the model in Ref. [46]. The total widths have a mass dependence, and Ref. [45] uses somewhat different mass values than suggested by the most recent lattice calculations [1]. Those final states marked with a dagger (†) are ideal for experimental exploration because there are relatively few stable particles in the final state or moderately narrow intermediate resonances that may reduce combinatoric background. (We consider η, η', and ω to be stable final state particles.)

	Approximate Mass (MeV)	J^{PC}	Total Width (MeV)		Relevant Decays	Final States
			PSS	IKP		
π_1	1900	1^{-+}	$80-170$	120	$b_1\pi^\dagger$, $\rho\pi^\dagger$, $f_1\pi^\dagger$, $a_1\eta$, $\eta'\pi^\dagger$	$\omega\pi\pi^\dagger$, $3\pi^\dagger$, 5π, $\eta 3\pi^\dagger$, $\eta'\pi^\dagger$
η_1	2100	1^{-+}	$60-160$	110	$a_1\pi$, $f_1\eta^\dagger$, $\pi(1300)\pi$	4π, $\eta 4\pi$, $\eta\eta\pi\pi^\dagger$
η_1'	2300	1^{-+}	$100-220$	170	$K_1(1400)K^\dagger$, $K_1(1270)K^\dagger$, $K^*K^\dagger$	$KK\pi\pi^\dagger$, $KK\pi^\dagger$, $KK\omega^\dagger$
b_0	2400	0^{+-}	$250-430$	670	$\pi(1300)\pi$, $h_1\pi$	4π
h_0	2400	0^{+-}	$60-260$	90	$b_1\pi^\dagger$, $h_1\eta$, $K(1460)K$	$\omega\pi\pi^\dagger$, $\eta 3\pi$, $KK\pi\pi$
h_0'	2500	0^{+-}	$260-490$	430	$K(1460)K$, $K_1(1270)K^\dagger$, $h_1\eta$	$KK\pi\pi^\dagger$, $\eta 3\pi$
b_2	2500	2^{+-}	10	250	$a_2\pi^\dagger$, $a_1\pi$, $h_1\pi$	4π, $\eta\pi\pi^\dagger$
h_2	2500	2^{+-}	10	170	$b_1\pi^\dagger$, $\rho\pi^\dagger$	$\omega\pi\pi^\dagger$, $3\pi^\dagger$
h_2'	2600	2^{+-}	$10-20$	80	$K_1(1400)K^\dagger$, $K_1(1270)K^\dagger$, $K_2^*K^\dagger$	$KK\pi\pi^\dagger$, $KK\pi^\dagger$

C. GlueX sensitivity to $s\bar{s}$ mesons

Recent studies of the capability of the baseline GlueX detector indicate that we will have adequate sensitivity to a number of final states containing kaons. Generically, these appear to be final states in which the recoil proton is reconstructed, as this provides the kinematic fit with the most power to discriminate among particle mass hypotheses. We discuss below the GlueX senstivity to a variety of final state topologies motivated by the physics topics in the preceding sections.

Table III provides information from models of hybrid mesons on the expected decay modes of exotic quantum-number states. The η_1', the h_0', and the h_2' all couple to the $KK\pi\pi$ final state, while both the η_1' and the h_2' are expected to couple to the $KK\pi$ final state. To study the GlueX sensitivity to these two final states, we have modeled two decay chains. For the $KK\pi$ state, we assume one of the kaons is a K_S, which leads to a secondary vertex and the $K^+\pi^-\pi^+\pi^-$ final state:

$$
\begin{aligned}
\eta_1'(2300) &\to K^*K_S \\
&\to (K^+\pi^-)(\pi^+\pi^-) \\
&\to K^+\pi^-\pi^+\pi^-.
\end{aligned}
\tag{1}
$$

For the $KK\pi\pi$ state we assume no secondary vertex:

$$
\begin{aligned}
h_2'(2600) &\to K_1^+K^- \\
&\to (K^*(892)\pi^+)K^- \\
&\to K^+K^-\pi^-\pi^+.
\end{aligned}
\tag{2}
$$

In addition to the exotic hybrid channels, there is an interest in non-exotic $s\bar{s}$ mesons. In order to study the sensitivity to conventional $s\bar{s}$ states, we consider an excitation of the normal ϕ meson, the known $\phi_3(1850)$, which decays to $K\bar{K}$

$$
\phi_3(1850) \to K^+K^-.
\tag{3}
$$

The detection efficiency of this state will be typical of ϕ-like states decaying to the same final state.

Finally, as noted in Section III B, the $Y(2175)$ state is viewed as a potential candidate for a non-exotic hybrid and has been reported in the decay mode

$$
\begin{aligned}
Y(2175) &\to \phi f_0(980) \\
&\to (K^+K^-)(\pi^+\pi^-).
\end{aligned}
\tag{4}
$$

While this is the same $KK\pi\pi$ state noted in reaction 2 above, the intermediate resonances make the kinematics of the final state particles different from the exotic decay channel noted above. Therefore, we simulate it explicitly.

The final-state kaons from the reactions 1 - 4 will populate the GlueX detectors differently, with different overlap of the region where the time-of-flight system can provide good K/π separation. Figure 5 shows the kinematics of these kaons and the overlap with the existing time-of-flight sensitivity.

A BDT analysis (see Section II C 2) has been used to study the capabilities of the baseline GlueX detector to identify the four reactions of interest. This study used the PYTHIA-simulated γp collisions from the large-scale data challenge as described in Section II B. Signal samples were obtained from PYTHIA events with the generated reaction topology, and the remainder of the inclusive photoproduction reactions were used as the background sample. A large number of discriminating variables were used in the BDT analysis, which generated a single classifier by combining the information from all of the input variables. (The BDT algorithms used are contained within ROOT in the TMVA package [47].)

In all cases we set the requirement on the BDT classifier in order to obtain a fixed final sample purity. For example, a purity of 90% implies a background at the 10% level. Any exotic signal in the spectrum would likely need to be larger than this background to be robust. There-
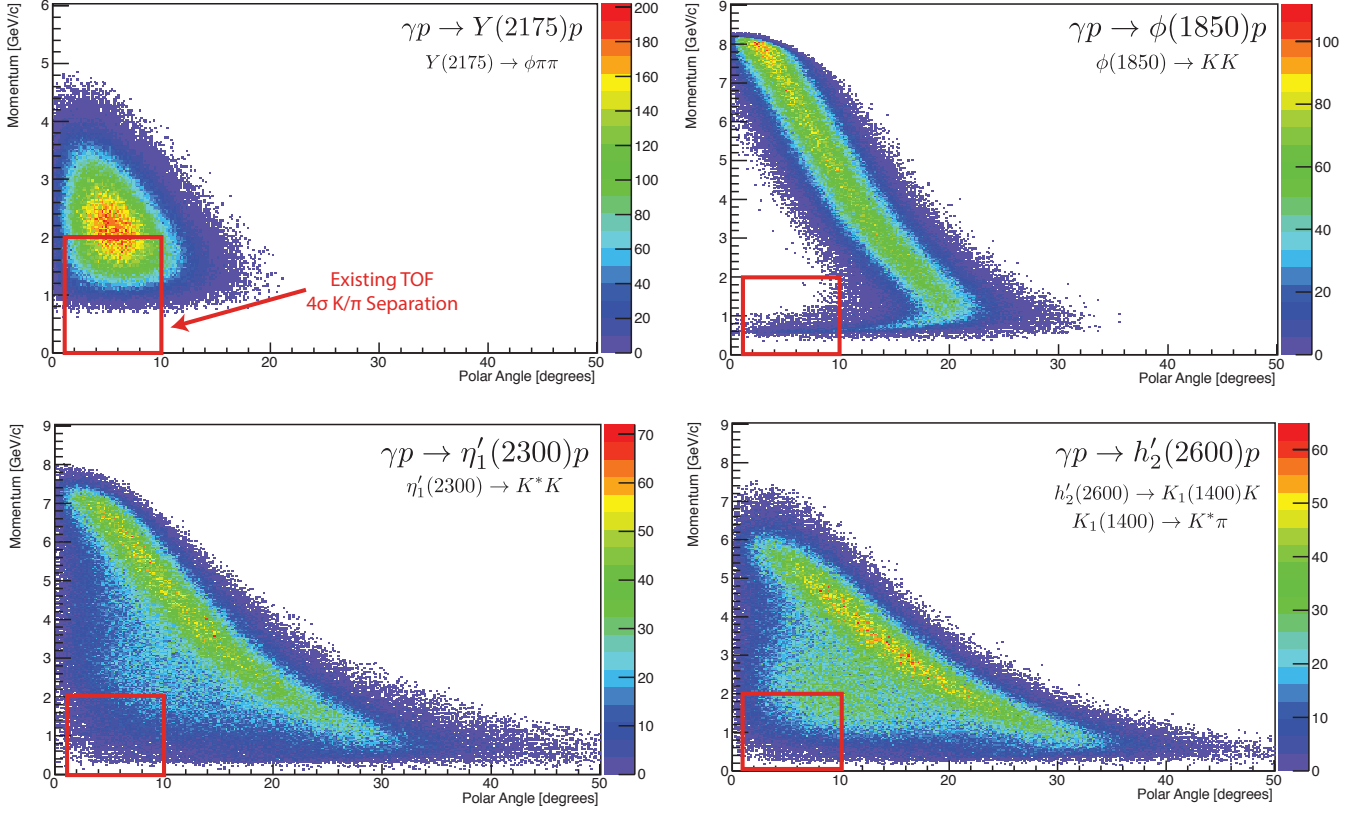
FIG. 5. Plots of particle density as a function of momentum and polar angle for all kaons in a variety of different production channels. Shown in solid (red) is the region of phase space where the existing time-of-flight (TOF) detector in GLUEX provides K/π discrimination at the four standard deviation level.

fore, with increased purity we have increased sensitivity to smaller signals, but also lower efficiency. In Table IV, we present the signal selection efficiencies (post reconstruction) for our four reactions of interest assuming the design resolution of the GLUEX tracking system. As noted earlier, these assume that the tracks have been reconstructed and do not include that efficiency. Historical evidence suggests that simulated resolutions are always more optimistic than what is attainable with the actual detector. To check the sensitivity of our conclusions to such a systematic error, we repeat the study while degrading the tracking resolution by 50%. At the 90% purity level, this degradation reduces the efficiency noticeably but not severely.

Finally, we have studied the resulting efficiency when we require a signal purity of 95%, which, for example, would be necessary to search for more rare final states. As can be seen in Table IV, increasing the desired purity noticeably reduces the efficiency: in two of the four topologies studied the efficiency drops by over 50% of itself as the desired purity is increased from 90% to 95%. This exposes the limit of what can be done with the baseline GLUEX hardware. Preliminary studies with supplemental kaon identification hardware (similar to those dis-

TABLE IV. Efficiencies for identifying several final states in GLUEX. The efficiencies do not include the reconstruction of the final state tracks.

Meson Decay	Tracking Resolution	Signal Purity	Selection Efficiency
$\phi_3(1850) \to K^+K^-$	Nominal	0.90	0.73
$Y(2175) \to \phi f_0(980)$	Nominal	0.90	0.53
$\eta'_1(2300) \to K^*K_S$	Nominal	0.90	0.32
$h'_2(2600) \to K_1^+K^-$	Nominal	0.90	0.26
$\phi_3(1850) \to K^+K^-$	Degraded	0.90	0.73
$Y(2175) \to \phi f_0(980)$	Degraded	0.90	0.49
$\eta'_1(2300) \to K^*K_S$	Degraded	0.90	0.31
$h'_2(2600) \to K_1^+K^-$	Degraded	0.90	0.25
$\phi_3(1850) \to K^+K^-$	Nominal	0.95	0.67
$Y(2175) \to \phi f_0(980)$	Nominal	0.95	0.31
$\eta'_1(2300) \to K^*K_S$	Nominal	0.95	0.15
$h'_2(2600) \to K_1^+K^-$	Nominal	0.95	0.09

cussed in our PAC 39 proposal) indicate that very high-purity samples are attainable with significantly improved efficiency. It is likely that studies of final states where the

background must be reduced below 10% will need additional particle identification hardware.

IV. Ξ BARYONS

The spectrum of multi-strange hyperons is poorly known, with only a few well-established resonances. Among the doubly-strange states, the two ground-state Cascades, the octet member $\Xi(1320)$ and the decuplet member $\Xi(1530)$, have four-star status in the PDG [11], with only four other three-star candidates. On the other hand, more than 20 N^* and Δ^* resonances are rated with at least three stars in the PDG. Of the six Ξ states that have at least a three-star rating in the PDG, only two are listed with weak experimental evidence for their spin-parity (J^P) quantum numbers: $\Xi(1530)\frac{3}{2}^+$ [48] and $\Xi(1820)\frac{3}{2}^-$ [49]. All other J^P assignments, including the J^P for the $\Xi(1320)$ ground state, are based on quark-model predictions. Flavor $SU(3)$ symmetry predicts as many Ξ resonances as N^* and Δ^* states combined, suggesting that many more Cascade resonances remain undiscovered. The three lightest quarks, u, d, and s, have 27 possible flavor combinations: $3\otimes3\otimes3 = 1\oplus8\oplus8'\oplus10$ and each multiplet is identified by its spin and parity, J^P. Flavor $SU(3)$ symmetry implies that the members of the multiplets differ only in their quark makeup, and that the basic properties of the baryons should be similar, although the symmetry is known to be broken by the strange-light quark mass difference. The octets consist of N^*, Λ^*, Σ^*, and Ξ^* states. We thus expect that for every N^* state, there should be a corresponding Ξ^* state *with similar properties.* Additionally, since the decuplets consist of Δ^*, Σ^*, Ξ^*, and Ω^* states, we also expect for every Δ^* state to find a decuplet Ξ^* with similar properties.

A. Ξ spectrum and decays

The Ξ hyperons have the unique feature of double strangeness: $|ssu\rangle$ and $|ssd\rangle$. If the confining potential is independent of quark flavor, the energy of spatial excitations of a given pair of quarks is inversely proportional to their reduced mass. This means that the lightest excitations in each partial wave are between the two strange quarks. In a spectator decay model, such states will not decay to the ground state Ξ and a pion because of orthogonality of the spatial wave functions of the two strange quarks in the excited state and the ground state. This removes the decay channel with the largest phase space for the lightest states in each partial wave, substantially reducing their widths. Typically, Γ_{Ξ^*} is about $10-20$ MeV for the known lower-mass resonances, which is $5-30$ times narrower than for N^*, Δ^*, Λ^*, and Σ^* states. These features, combined with their isospin of $1/2$, render possible a wide-ranging program on

the physics of the Cascade hyperon and its excited states. Until recently, the study of these hyperons has centered on their production in K^-p reactions; some Ξ^* states were found using high-energy hyperon beams. Photoproduction appears to be a very promising alternative. Results from earlier kaon beam experiments indicate that it is possible to produce the Ξ ground state through the decay of high-mass hyperon and Ξ states [50–52]. It is therefore possible to produce Ξ resonances through t-channel photoproduction of hyperon resonances using the photoproduction reaction $\gamma p \to KK\,\Xi^{(*)}$ [23, 24].

In briefly summarizing a physics program on Cascades, it would be interesting to see the lightest excited Ξ states in certain partial waves decoupling from the $\Xi\pi$ channel, confirming the flavor independence of confinement. Measurements of the isospin splittings in spatially excited Ξ states are also possible for the first time. Currently, these splittings, like $n-p$ or $\Delta^0 - \Delta^{++}$, are only available for the octet and decuplet ground states, but are hard to measure in excited N, Δ and Σ, Σ^* states, which are very broad. The lightest Cascade baryons are expected to be narrower, and measuring the $\Xi^- - \Xi^0$ splitting of spatially excited Ξ states remains a strong possibility. These measurements are an interesting probe of excited hadron structure and would provide important input for quark models, which describe the isospin splittings by the u- and d-quark mass difference as well as by the electromagnetic interactions between the quarks.

B. GlueX sensitivity to Ξ states

The Ξ's appear to be produced via t-channel exchanges that result in the production of a hyperon Y^* at the lower vertex which then decays to $\Xi^{(*)}K$. Most of the momentum of the beam is transferred to a forward-going kaon that is produced at the upper vertex.

The Ξ octet ground states (Ξ^0, Ξ^-) will be challenging to study in the GlueX experiment via exclusive t-channel (meson exchange) production. The typical final states for these studies,

$$\gamma p \to K Y^* \to K^+ (\,\Xi^- K^+\,),$$
$$K^+ (\,\Xi^0 K^0\,),$$
$$K^0 (\,\Xi^0 K^+\,), \qquad (5)$$

have kinematics for which the baseline GlueX detector has very low acceptance due to the high-momentum forward-going kaon and relatively low-momentum pions produced in the Ξ decay.

However, the production of the Ξ decuplet ground state, $\Xi(1530)$, and other excited Ξ's decaying to $\Xi\pi$ results in a lower momentum kaon at the upper vertex, and these heavier Ξ states produce higher momentum pions in their decays. GlueX will be able to search for and

study excited Ξ's in the reactions

$$
\begin{aligned}
\gamma p \;\to\; K\,Y^* \;\to\;\; & K^+\,(\,\Xi\,\pi\,)\,K^0, \\
& K^+\,(\,\Xi\,\pi\,)\,K^+, \\
& K^0\,(\,\Xi\,\pi\,)\,K^+\,.
\end{aligned}
\tag{6}
$$

The lightest excited Ξ states are expected to decouple from $\Xi\pi$ and can be searched for and studied also in their decays to $\Lambda\bar{K}$ and $\Sigma\bar{K}$:

$$
\begin{aligned}
\gamma p \;\to\; K\,Y^* \;\to\;\; & K^+\,(\,\bar{K}\Lambda\,)_{\Xi^{-*}}\,K^+, \\
& K^+\,(\,\bar{K}\Lambda\,)_{\Xi^{0*}}\,K^0, \\
& K^0\,(\,\bar{K}\Lambda\,)_{\Xi^{0*}}\,K^+,
\end{aligned}
\tag{7}
$$

$$
\begin{aligned}
\gamma p \;\to\; K\,Y^* \;\to\;\; & K^+\,(\,\bar{K}\Sigma\,)_{\Xi^{-*}}\,K^+, \\
& K^+\,(\,\bar{K}\Sigma\,)_{\Xi^{0*}}\,K^0, \\
& K^0\,(\,\bar{K}\Sigma\,)_{\Xi^{0*}}\,K^+.
\end{aligned}
\tag{8}
$$

We have simulated the production of the $\Xi^-(1320)$ and $\Xi^-(1820)$ resonances to better understand the kinematics of these reactions. The photoproduction of the $\Xi^-(1320)$ decaying to $\pi^-\Lambda$ and of the $\Xi^-(1820)$ decaying to ΛK^- are shown in Fig. 6. These reactions result in $K^+K^+\pi^-\pi^-p$ and $K^+K^+K^-\pi^-p$ final states, respectively. Reactions involving excited Ξ states have lower-momentum forward-going kaons, making them more favorable for study without supplemental particle ID hardware in the forward direction. In addition, there is more energy available on average to the Ξ decay products, which results in a better detection efficiency for the produced pions.

Using a BDT for signal selection, we have studied the specific reaction

$$
\gamma p \to K^+\Xi^-(1820)K^+\,,
$$

with the subsequent decay of the Ξ via

$$
\begin{aligned}
\Xi^-(1820) &\to \Lambda K^- \\
&\to (p\pi^-)K^-\,.
\end{aligned}
$$

The signal selection efficiencies (post-reconstruction) are shown in Table V. As with the mesons, we find the efficiency should be adequate for conducting a study of excited Ξ states using the existing GLUEX hardware. Detailed studies of the production, especially of the ground state Ξ's, and a parity measurement will likely require enhanced kaon identification in the forward direction, as presented in our PAC 39 proposal.

TABLE V. Selection efficiencies for identifying the $\Xi^-(1820)$. The efficiencies do not include the reconstruction efficiency of the final state tracks.

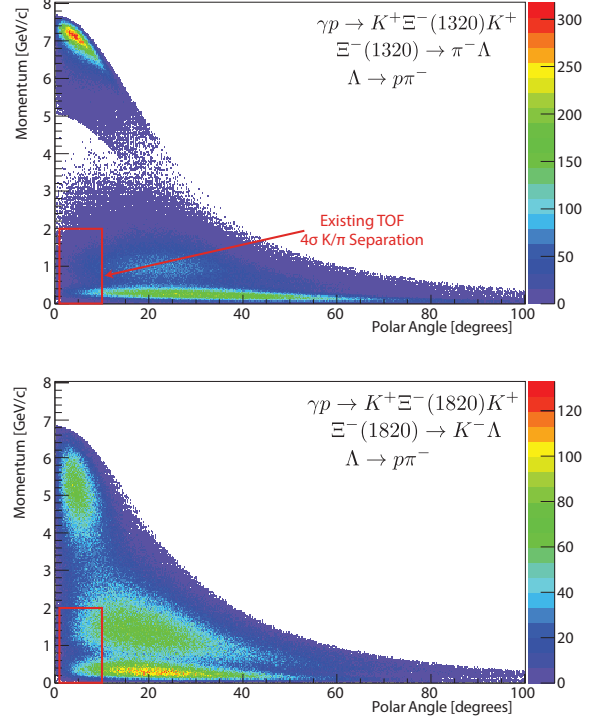| Baryon	Tracking Resolution	Signal Purity	Selection Efficiency
$\Xi^-(1820)$	Nominal	0.90	0.36
$\Xi^-(1820)$	Nominal	0.95	0.27

FIG. 6.   Generated momentum versus polar angle for all tracks in the simulated reactions (top) $\gamma p \to K^+\,\Xi^-(1320)K^+$ and (bottom) $\gamma p \to K^+\,\Xi^-(1820)K^+$. The three high-density regions in each plot are populated with, from lowest to highest momentum, pions, kaons and protons, and kaons.

V.   GLUEX HARDWARE AND BEAM TIME REQUIREMENTS

In order to maximize the discovery capability of GLUEX, an increase in statistical precision beyond that expected from initial running is needed. In this section, we detail those needs. To maximize sensitivity, we propose a gradual increase in the photon flux towards the GLUEX design of 10^8 γ/s in the peak of the coherent bremsstrahlung spectrum (8.4 GeV $< E_\gamma <$ 9.0 GeV). Yield estimates, assuming an average flux of 5×10^7 γ/s, are presented. In order to minimize the bandwidth to disk and ultimately enhance analysis efficiency, we propose the addition of a level-three software trigger to the GLUEX data acquisition system. The GLUEX detector is designed to handle a rate of 10^8 γ/s; however, the optimum photon flux for taking data will depend on the beam condition and pileup at high luminosity and needs to be studied under realistic experimental conditions. If our extraction of amplitudes is not limited by statistical uncertainties, we may optimize the flux to reduce systematic errors.

A. Level-three trigger

The energy spectrum of photons striking the target ranges from near zero to the full 12 GeV incident electron energy. For physics analyses, one is primarily interested in only those events in the coherent peak around 9 GeV, where there is a signal in the tagger that determines the photon energy. At a rate of 10^7 γ/s, the 120 μb total hadronic cross section at 9 GeV corresponds to a tagged hadronic event rate of about 1.5 kHz. Based on knowledge of the inclusive photoproduction cross section as a function of energy, calculations of the photon intensity in the region outside the tagger acceptance, and estimates for the trigger efficiency, a total trigger rate of about 20 kHz is expected. At a typical raw event size of 15 kB, the expected data rate of 300 MB/s will saturate the available bandwidth to disk; rates higher than 10^7 γ/s cannot be accommodated with the current data acquisition configuration.

For the high-intensity running, we propose the development of a level-three software trigger to loosely skim events that are consistent with a high energy γp collision. The events of interest will be characterized by high-momentum tracks and large energy deposition in the calorimeter. Matching observed energy with a tagger hit is a task best suited for software algorithms like those used in physics analysis. It is expected that a processor farm can analyze multiple events in parallel, providing a real time background rejection rate of at least a factor of ten. While the exact network topology and choice of hardware will ultimately depend on the speed of the algorithm, at 10^8 γ/s the system will need to accommodate 3 GB/s input from data crates, separate data blocks into complete events, and output the accepted events to disk at a rate of < 300 MB/s. The software trigger has the added advantage of increasing the concentration of tagged γp collision events in the output stream, which better optimizes use of disk resources and enhances analysis efficiency. Members of the GLUEX collaboration have developed and implemented the software trigger for the LHCb experiment, which is one of the most sophisticated software triggers ever developed [38, 39]. We expect to benefit greatly from this expertise in developing an optimal level-three trigger for GLUEX.

The present baseline data acquisition system has been carefully developed so that a level-three software trigger can be easily accommodated in the future. We expect to begin prototyping the level-three trigger using surplus computing hardware during the initial phases of GLUEX running. This early testing of both algorithms and hardware will allow us to specify our resource needs with good accuracy in advance of the proposed Phase IV running.

A simple estimate indicates that the implementation of a level-three trigger easily results in a net cost savings rather than a burden. Assuming no bandwidth limitations, if we write the entire unfiltered high-luminosity data stream to tape, the anticipated size is about 30 petabytes per year [2]. Estimated media costs for storage of this data at the time of running would be \$300K, assuming that no backup is made. A data volume of this size would require the acquisition of one or more additional tape silos at a cost of about \$250K each. Minimum storage costs for a multi-year run will be nearing one million dollars. Conversely, if we assume a level-three trigger algorithm can run a factor of ten faster than our current full offline reconstruction, then we can process events at a rate of 100 Hz per core. The anticipated peak high luminosity event rate of 200 kHz would require 2000 cores, which at *today's costs* of 64-core machines would be about \$160K. Even if a factor of two in computing is added to account for margin and data input/output overhead, the cost is significantly lower than the storage cost. Furthermore, it is a fixed cost that does not grow with additional integrated luminosity, and it reduces the processing cost of the final stored data set when a physics analysis is performed on the data.

B. Desired beam time and intensity

There are several considerations in determining how much data one needs in any particular final state. In order to perform an amplitude analysis of the final state particles (necessary for extracting the quantum numbers of the produced resonances), one typically separates the data into bins of momentum transfer to the nucleon t and resonance mass M_X. The number of bins in t could range from one to greater than ten, depending on the statistical precision of the data; a study of the t-dependence, if statistically permitted, provides valuable information on the production dynamics of particular resonances. One desires to make the mass bins as small as possible in order to maximize sensitivity to states that have a small total decay width; however, it is not practical to use a bin size that is smaller than the resolution of M_X, which is on the order of 10 MeV/c^2. In each bin of t and M_X, one then needs enough events to perform an amplitude analysis, which is about 10^4. Therefore, our general goal is to reach a level of at least 10^4 events per 10 MeV/c^2 mass bin. With more statistics, we can divide the data into bins of t to study the production mechanism; with fewer statistics, we may merge mass bins, which ultimately degrades the resolution with which we can measure the masses and widths of the produced resonances.

In order to estimate the total event yield for various reactions of interest, we assume 200 PAC days of beam for the proposed Phase IV running with 80% of the delivered beam usable for physics analysis. The average

---

[2] This is at the GLUEX design intensity of 10^8 γ/s, which is higher than our Phase IV average rate of 5×10^7 by a factor of two; however, other factors that would increase the data volume, such as event size increases due to higher-than-estimated noise, have not been included.

Phase IV intensity is assumed to be 5×10^7 γ/s in the coherent bremsstrahlung peak. This represents an integrated yield of events that is approximately one order of magnitude larger than our approved Phase II and III running, which utilizes 90 PAC days of beam for physics analysis[3] at an average intensity of 10^7 γ/s in the coherent peak. Table VI summarizes the various running configurations.

Below we present two independent estimates of event yields to justify our request for 200 PAC days of beam. Both reach similar conclusions: the proposed run would provide sufficient statistics to conduct an initial amplitude analysis of the mass spectrum for several select $s\bar{s}$ meson decay modes. In addition, the resulting order-of-magnitude increase in statistical precision will allow a more detailed exploration of those topologies such as $\eta'\pi$, $b_1\pi$, or $f_1\pi$ that may be statistically limited in the initial GLUEX running. Finally, the spectrum of Ξ baryons can also be studied with high statistical precision.

1. Meson yields based on cross section estimates

One can estimate the total number of observed events, N_i, in some stable final state by

$$N_i = \epsilon_i \sigma_i n_\gamma n_t T, \tag{9}$$

where ϵ_i and σ_i are the detection efficiency and photoproduction cross section of the final state i, n_γ is the rate of incident photons on target, n_t is the number of scattering centers per unit area, and T is the integrated live time of the detector. For a 30 cm LH$_2$ target, n_t is 1.26 b^{-1}. (A useful rule of thumb is that at $n_\gamma = 10^7$ γ/s a 1 μb cross section will result in the production of about 10^6 events per day.) It is difficult to estimate the production cross section for many final states since data in the GLUEX energy regime are sparse. (For a compendium of photoproduction cross sections, see Ref. [53].) Table VII lists key final states for initial exotic hybrid searches along with assumed production cross sections[4].

Photoproduction of mesons at 9 GeV proceeds via peripheral production (sketched in the inset of Fig. 7). The production can typically be characterized as a function of $t \equiv (p_X - p_\gamma)^2$, with the production cross section proportional to $e^{-\alpha|t|}$. The value of α for measured reactions ranges from 3 to 10 GeV^{-2}. This t-dependence, which is unknown for many key GLUEX reactions, results in a suppression of the rate at large values of $|t|$, which, in turn,
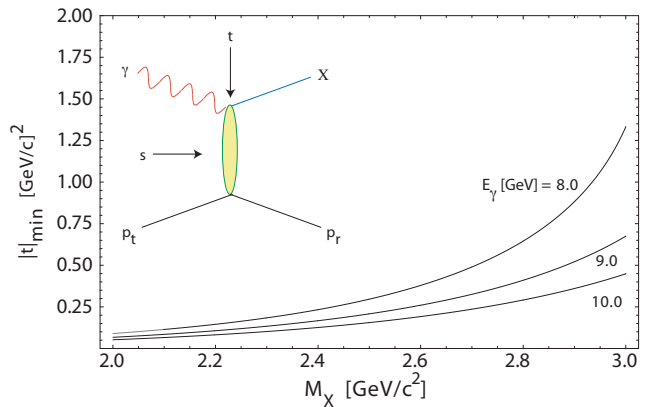

FIG. 7. Dependence of $|t|_{\min}$ on the mass of the outgoing meson system M_X. The lines indicate incident photon energies of 8.0, 9.0, and 10.0 GeV.

suppresses the production of high mass mesons. Figure 7 shows the minimum value of $|t|$ as a function of the produced meson mass M_X for a variety of different photon energies. The impact of this kinematic suppression on a search for heavy states is illustrated in Figure 8, where events are generated according to the t distributions with both $\alpha = 5$ (GeV/c)$^{-2}$ and 10 (GeV/c)$^{-2}$ and uniform in M_X. Those that are kinematically allowed ($|t| > |t|_{\min}$) are retained. The y-axis indicates the number of events in 10 MeV/c^2 mass bins, integrated over the allowed region in t, and assuming a total of 3×10^7 events are collected. The region above $M_X = 2.5$ GeV/c^2, where one would want to search for states such as the h_2 and h_2', contains only about 5% of all events due to the suppression of large $|t|$ that is characteristic of peripheral photoproduction.

To estimate our total yield in various final states, we assume the detection efficiency for protons, pions, kaons, and photons to be 70%, 80%, 40%, and 80%, respectively. Of course, the true efficiencies are dependent on software algorithms, kinematics, multiplicity, and other variables; however, the dominant uncertainty in yield estimates is not efficiency but cross section. These assumed efficiencies roughly reproduce signal selection efficiencies in detailed simulations of $\gamma p \to \pi^+\pi^-\pi^+ n$, $\gamma p \to \eta\pi^0 p$, $\gamma p \to b_1^\pm \pi^\mp p$, and $\gamma p \to f_1\pi^0 p$ performed by the collaboration, as well as the BDT selection efficiencies presented earlier. Table VII provides an estimate of the detected yields for various topologies for our proposed Phase IV run. If we take the $KK\pi$ channel as an example, Figure 8 demonstrates that, under some assumptions about the production, the proposed run yields enough statistics to just meet our goal of 10^4 events per mass bin in the region where $s\bar{s}$ exotics are expected to reside.

---

[3] We plan to utilize 30 of the 120 approved PAC days for the Phase I commissioning of the detector.

[4] Some estimates are based on actual data from Ref. [53] for cross sections at a similar beam energy, while others are crudely estimated from the product of branching ratios of heavy meson decays, *i.e.*, a proxy for light meson hadronization ratios, and known photoproduction cross sections.

TABLE VI. A table of relevant parameters for the various phases of GLUEX running.

	Approved			*Proposed*
	Phase I	Phase II	Phase III	Phase IV
Duration (PAC days)	30	30	60	200
Minimum electron energy (GeV)	10	11	12	12
Average photon flux (γ/s)	10^6	10^7	10^7	5×10^7
Average beam current (nA)	50 - 200[a]	220	220	1100
Maximum beam emittance (mm·μr)	50	20	10	10
Level-one (hardware) trigger rate (kHz)	2	20	20	200
Raw Data Volume (TB)	60	600	1200	2300[b]

[a] An amorphous radiator may be used for some commissioning and later replaced with a diamond.
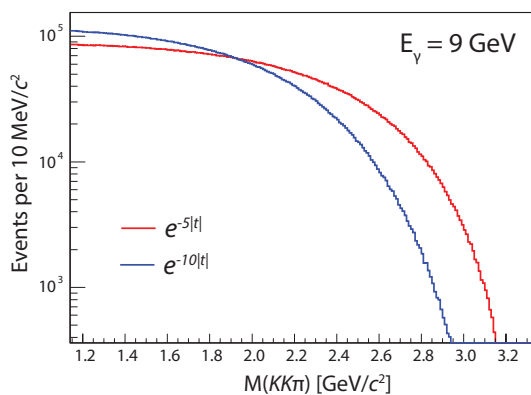[b] This volume assumes the implementation of the proposed level-three software trigger.

FIG. 8. A figure showing the number of expected events per 10 MeV/c^2 bin in the $KK\pi$ invariant mass distribution, integrating over all allowed values of t, and assuming 10^7 events in total are detected. No dependence on $M(KK\pi)$ is assumed, although, in reality, the mass dependence will likely be driven by resonances. Two different assumptions for the t dependence are shown. The region above 2.5 GeV/c^2 represents about 8% (2%) of all events for the $\alpha = 5(10)$ (GeV/c)$^{-2}$ values.

TABLE VII. A table of hybrid search channels, estimated cross sections, and approximate numbers of observed events for the proposed Phase IV running. See text for a discussion of the underlying assumptions. The subscripts on ω, η, and η' indicate the decay modes used in the efficiency calculations. If explicit charges are not indicated, the yields represent an average over various charge combinations.

Final State	Cross Section (μb)	Proposed Phase IV ($\times 10^6$ events)
$\pi^+\pi^-\pi^+$	10	3000
$\pi^+\pi^-\pi^0$	2	600
$KK\pi\pi$	0.5	40
$KK\pi$	0.1	10
$\omega_{3\pi}\pi\pi$	0.2	40
$\omega_{\gamma\pi}\pi\pi$	0.2	6
$\eta_{\gamma\gamma}\pi\pi$	0.2	30
$\eta_{\gamma\gamma}\pi\pi\pi$	0.2	20
$\eta'_{\gamma\gamma}\pi$	0.1	1
$\eta'_{\eta\pi\pi}\pi$	0.1	3

2. Meson yields based on PYTHIA simulation

We have also used PYTHIA to simulate the expected yields of various hadronic final states. PYTHIA reproduces known photoproduction cross sections relatively well; therefore, it is expected to be an acceptable estimator of the production rates of various topologies where we would like to search for new mesons. Using the large 5×10^9 event inclusive-photoproduction PYTHIA sample, we can analyze the signal yield when we attempt to reconstruct and select various final state topologies. The signal selection is performed using a BDT, as discussed earlier, with a goal of 90% signal purity. We place loose requirements on the invariant masses of the intermediate resonances. The measured yield after reconstruction and selection can then be scaled to estimate the number of reconstructed signal events that our Phase IV running would produce. In Table VIII we show the various topologies studied. In addition, we measure the yield in a region of meson candidate X invariant mass to estimate the statistical precision of an amplitude analysis in that region. The number of events per 10 MeV/c^2 mass bin is listed, and we observe that we meet our goal of 10^4 events per bin in most topologies. The K^*K_S yield in Table VIII also loosely agrees with that in Figure 8, and the ratio of K_1K to K^*K roughly matches that obtained by estimated cross sections and efficiencies as shown in Table VII.

TABLE VIII. PYTHIA-predicted numbers of events for various exclusive final states in a mass range appropriate for searching for various mesons. Estimates are based of 200 PAC days at 80% uptime at an average intensity of $5 \times 10^7 \gamma$/s. Events per 10 MeV/c^2 is an estimate of the number of events available for an amplitude analysis in each mass bin.

Meson of Interest (X)	Reaction Topology	Mass Range [MeV/c^2] $M_X^{\min}$	$M_X^{\max}$	Signal Yield [10^6]	Events per 10 MeV/c^2 [10^4]
$h'_2(2600)$	$\gamma p \to (K_1(1400)K)_X p$	2415	2785	1.5	4.0
	$K_1 \to K^* \pi$				
	$K^* \to K\pi$				
$\eta'_1(2300)$	$\gamma p \to (K^* K_S)_X p$	2000	2600	0.46	1.5
	$K^* \to K^{\pm}\pi^{\mp}$				
	$K_S \to \pi^+\pi^-$				
$\phi_3(1850)$	$\gamma p \to (K^+K^-)_X p$	1720	1980	5.3	21
$Y(2175)$	$\gamma p \to (\phi f_0(980))_X p$	2060	2290	0.12	0.52
	$\phi \to K^+K^-$				
	$f_0(980) \to K^+K^-$				

3. Ξ yields

Existing knowledge of Ξ photoproduction can be used to estimate the expected yields of Ξ states. Recent CLAS data for the $\Xi(1320)$ are consistent with t-slope values ranging from 1.11 to 2.64 (GeV/c)$^{-2}$ for photon energies between 2.75 and 3.85 GeV [24]. Values for excited Cascades are not well known, but a recent unpublished CLAS analysis of a high-statistics data sample (JLab proposal E05-017) indicates that the t-slope value flattens out above 4 GeV at a value of about 1.7 (GeV/c)$^{-2}$ [54]. We have used a value of 1.4 (GeV/c)$^{-2}$ for the $\Xi^-(1320)$ and 1.7 (GeV/c)$^{-2}$ for the $\Xi^-(1820)$ in our simulations at 9 GeV. The most recent published CLAS analysis [24] has determined a total cross section of about 15 nb and 2 nb for the $\Xi^-(1320)$ and $\Xi^-(1530)$, respectively, at $E_\gamma = 5$ GeV. An unpublished analysis shows that the total cross section levels out above 3.5 GeV, but the energy range is limited at 5.4 GeV [54]. A total number of about 20,000 $\Xi^-(1320)$ events was observed for the energy range $E_\gamma \in [2.69, 5.44]$ GeV.

The BDT analysis carried out using $K^+K^+K^-\Lambda$ PYTHIA signal events suggests that the proposed GlueX run will result in a yield of about 90,000 of these events with 90% purity for $K^-\Lambda$ invariant mass in the $\Xi(1820)$ mass region. Estimates using Eq. (9) lead us to expect yields of about $800,000$ $\Xi^-(1320)$ and $100,000$ $\Xi^-(1530)$ events. Such high statistics samples of exclusively reconstructed Ξ final states greatly enhance the possibility of determining the spin and parity of excited states.

In summary, we request a production run consisting of 200 days of beam time at an average intensity of 5×10^7 γ/s for production Phase IV running of the GlueX experiment. It is anticipated that the Phase IV intensity will start around 10^7 γ/s, our Phase III intensity, and increase toward the GlueX design goal of 10^8 γ/s as we understand the detector capability for these high rates based on the data acquired at 10^7 γ/s. The data sample acquired will provide an order of magnitude improvement in statistical precision over the initial Phase II and III running of GlueX, which will allow an initial study of high-mass states containing strange quarks and an exploration of the Ξ spectrum.

VI. SUMMARY

We propose an expansion of the present baseline GlueX experimental program to include an order-of-magnitude higher statistics by increasing the average tagged photon intensity by a factor of five and the beam time by a factor of two. The increase in intensity necessitates the implementation of the GlueX level-three software trigger. The program requires 200 days of beam time with 9 GeV tagged photons at an average intensity of 5×10^7 γ/s. We have demonstrated that the baseline GlueX detector design is capable of reconstructing particular final state topologies that include kaons. While the acceptance and purity may be limited without the addition of supplemental kaon identification hardware, the proposed run will provide a level of statistical precision sufficient to make an initial study of meson states with an $s\bar{s}$ component and to search for excited doubly-strange Ξ-baryon states.

[1] J. J. Dudek, Phys. Rev. D **84**, 074023 (2011).

[2] GlueX Collaboration, "Mapping the Spectrum of Light Quark Mesons and Gluonic Excitations with Linearly Po-

larized Protons," *Presentation to PAC 30*, (2006). Available at: *http://www.gluex.org/docs/pac30_proposal.pdf*

[3] GLUEX Collaboration, "The GLUEX Experiment in Hall D," *Presentation to PAC 36*, (2010). Available at: *http://www.gluex.org/docs/pac36_update.pdf*

[4] GLUEX Collaboration, "A study of meson and baryon decays to strange final states with GLUEX in Hall D," *Presentation to PAC 39*, (2012). Available at: *http://www.gluex.org/docs/pac39_proposal.pdf*

[5] J. J. Dudek, R. G. Edwards, M. J. Peardon, D. G. Richards and C. E. Thomas, Phys. Rev. Lett. **103**, 262001 (2009).

[6] J. J. Dudek, R. G. Edwards, M. J. Peardon, D. G. Richards and C. E. Thomas, Phys. Rev. D **82**, 034508 (2010).

[7] J. J. Dudek, R. G. Edwards, B. Joo, M. J. Peardon, D. G. Richards and C. E. Thomas, Phys. Rev. D **83**, 111502 (2011).

[8] R. G. Edwards, J. J. Dudek, D. G. Richards and S. J. Wallace, Phys. Rev. D **84**, 074508 (2011).

[9] J. J. Dudek and R. G. Edwards, Phys. Rev. D **85**, 054016 (2012).

[10] R. G. Edwards, N. Mathur, D. G. Richards and S. J. Wallace, Phys. Rev. D **87**, 054506 (2013) [arXiv:1212.5236 [hep-ph]].

[11] J. Beringer *et al.* [Particle Data Group Collaboration], Phys. Rev. D **86**, 010001 (2012).

[12] M. Ablikim *et al.* [BESIII Collaboration], Phys. Rev. Lett. **106**, 072002 (2011).

[13] G. S. Adams *et al.* [CLEO Collaboration], Phys. Rev. D **84**, 112009 (2011).

[14] E. I. Ivanov *et al.* [E852 Collaboration], Phys. Rev. Lett. **86**, 3977 (2001).

[15] C. A. Meyer and Y. Van Haarlem, Phys. Rev. C **82**, 025208 (2010).

[16] B. Aubert *et al.* [BABAR Collaboration], Phys. Rev. Lett. **95**, 142001 (2005).

[17] T. E. Coan *et al.* [CLEO Collaboration], Phys. Rev. Lett. **96**, 162003 (2006).

[18] Q. He *et al.* [CLEO Collaboration], Phys. Rev. D **74**, 091104 (2006).

[19] C. Z. Yuan *et al.* [Belle Collaboration], Phys. Rev. Lett. **99**, 182004 (2007).

[20] B. Aubert *et al.* [BABAR Collaboration], Phys. Rev. D **74**, 091103 (2006).

[21] M. Ablikim *et al.* [BES Collaboration], Phys. Rev. Lett. **100**, 102003 (2008).

[22] C. P. Shen *et al.* [Belle Collaboration], Phys. Rev. D **80**, 031101 (2009).

[23] J. W. Price *et al.* [CLAS Collaboration], Phys. Rev. C **71**, 058201 (2005).

[24] L. Guo *et al.*, Phys. Rev. C **76**, 025208 (2007).

[25] J. J. Dudek and E. Rrapaj, Phys. Rev. D **78**, 094504 (2008).

[26] L. Liu *et al.*, arXiv:1204.5425 [hep-ph].

[27] Y. Van Haarlem *et al.*, Nucl. Instrum. Meth. A **622**, 142 (2010).

[28] A. Brunner *et al.*, Nucl. Instrum. Meth. A **414**, 466 (1998).

[29] K. Moriya *et al.*, arXiv:1304.499[physics-ins.det] (submitted to Nucl. Instrum. Meth. A) (2013).

[30] David Nathan Brown, Sergei Gerassimov, Chris Jones, Martin Purschke, and Torre Wenaus, "Report of the 12 GeV Software and Computing Review," GlueX-doc-2055, September 2012.

[31] G. S. Adams *et al.* [E852 Collaboration], Phys. Rev. Lett. **81**, 5760 (1998).

[32] A. R. Dzierba *et al.*, Phys. Rev. D **73**, 072001 (2006).

[33] M. Alekseev *et al.* [COMPASS Collaboration], Phys. Rev. Lett. **104**, 241803 (2010).

[34] M. Nozar *et al.* [CLAS Collaboration], Phys. Rev. Lett. **102**, 102002 (2009).

[35] I. Senderovich, Ph.D. Thesis (unpublished), University of Connecticut (2012).

[36] L. Brieman *el al.*, *Classification and regression trees*, Wadsworth International Group, Belmont, California (1984).

[37] R. Aaij *et al.* [LHCb Trigger Group], *The LHCb trigger and its performance*, Submitted to JINST. [arxiv:1211.3055]

[38] V. Gligorov and M. Williams, *Efficient, reliable and fast high-level triggering using a bonsai boosted decision tree*, JINST **8**, P02013 (2013).

[39] B.P. Roe *et al.*, *Boosted decision trees as an alternative to artificial neural networks for particle identification*, Nucl.Instrum.Meth. A **543**, 577 (2005).

[40] F. E. Close and P. R. Page, Phys. Lett. B **628**, 215 (2005).

[41] S. -L. Zhu, Phys. Lett. B **625**, 212 (2005).

[42] E. Kou and O. Pene, Phys. Lett. B **631**, 164 (2005).

[43] X. -Q. Luo and Y. Liu, Phys. Rev. D **74**, 034502 (2006) [Erratum-ibid. D **74**, 039902 (2006)].

[44] G. -J. Ding and M. -L. Yan, Phys. Lett. B **657**, 49 (2007).

[45] P. R. Page, E. S. Swanson and A. P. Szczepaniak, Phys. Rev. D **59**, 034016 (1999).

[46] N. Isgur, R. Kokoski and J. E. Paton, Phys. Rev. Lett. **54**, 869 (1985).

[47] A. Hoecker, P. Speckmayer, J. Stelzer, J. Therhaag, E. von Toerne, and H. Voss, *TMVA: Toolkit for Multivariate Data Analysis*, PoS A CAT 040 (2007).

[48] B. Aubert *et al.* [BABAR Collaboration], Phys. Rev. D **78**, 034008 (2008).

[49] S. F. Biagi *et al.*, Z. Phys. C **34**, 175 (1987).

[50] R. D. Tripp *et al..*, Nucl. Phys. B **3**, 10 (1967).

[51] G. Burgun *et al.*, Nucl. Phys. B **8**, 447 (1968).

[52] P. J. Litchfield *et al.*, Nucl. Phys. B **30**, 125 (1971).

[53] A. Baldini, V. Flaminio, W. G. Moorhead, D. R. O. Morrison and H. Schopper, (Ed.), "Numerical Data And Functional Relationships In Science And Technology. Grp. 1: Nuclear And Particle Physics. Vol. 12: Total Cross-sections For Reactions Of High-energy Particles (including Elastic, Topological, Inclusive And Exclusive Reactions). Subvol," BERLIN, GERMANY: SPRINGER (1988) 409 P. (LANDOLT-BOERNSTEIN. NEW SERIES, 1/12B)

[54] John Theodore Goetz, Ph.D. Thesis, University of California, Los Angeles, 2010 (unpublished).